

OPTIMIZATION OF THE LAYOUT OF LARGE WIND FARMS USING
A GENETIC ALGORITHM

by

ANSHUL MITTAL

Submitted in partial fulfillment of the requirements

For the degree of Master of Science

Department of Mechanical and Aerospace Engineering

CASE WESTERN RESERVE UNIVERSITY

May, 2010

CASE WESTERN RESERVE UNIVERSITY
SCHOOL OF GRADUATE STUDIES

We hereby approve the thesis/dissertation of

ANSHUL MITTAL

candidate for the MASTER OF SCIENCE degree *.

(signed) J. IWAN D. ALEXANDER
(chair of the committee)

ALEXIS R. ABRAMSON

JAIKRISHNAN R. KADAMBI

JOSEPH M. PRAHL

(date) 24 February, 2010

*We also certify that written approval has been obtained for any proprietary material contained therein.

Copyright © 2010 by Anshul Mittal

All rights reserved

Table of Contents

Table of Contents

List of Tables

List of Figures

Nomenclature

Abstract

Chapter 1 Introduction

1.1 Overview	1
1.2 Wake Models	3
1.2.1 Analytical Wake Models	3
1.2.2 Computational Wake Models	5
1.3 Performance of Wake models compared to data from wind farms	6
1.4 Optimization of turbine placement in a wind farm	8

Chapter 2 Problem Description

2.1 Wind Regimes	12
2.2 Factors in Wind Farm Design and Assumptions	13
2.3 Cost Model	17
2.4 The Jensen's Wake Model	19
2.5 Power Calculation	23
2.6 Optimization Process	24

2.6.1	Initialization	24
2.6.2	The Genetic Algorithm Solver or ‘ga’ solver	25
2.6.3	Post-processing	26
Chapter 3	Results and Discussion	
3.1	Case 1: Constant Wind Speed and Fixed Wind Direction	28
3.1.1	Results from previous studies	28
3.1.2	Results from WFOG with coarse grid spacing	32
3.1.3	Results from WFOG with fine grid spacing	37
3.2	Case 2: Constant Wind Speed and Variable Wind Direction	44
3.2.1	Results from previous studies	44
3.2.2	Results from WFOG with fine grid spacing	47
3.3	Case 3: Variable Wind Speed and Variable Wind Direction	51
3.3.1	Results from previous studies	52
3.3.2	Results from WFOG with fine grid spacing	55
Chapter 4	Conclusions and Recommendations	
4.1	Conclusions	59
4.2	Recommendations	59
Appendix		61
Bibliography		78

List of Tables

Table 3.1	Case 1: Previous studies: reported results and recomputed using WFOG	30
Table 3.2	Results for optimal layout from WFOG for Case 1	40
Table 3.3	Results for sub-optimal layouts from WFOG for Case 1	43
Table 3.4	Case 2: Previous studies: reported results and recomputed using WFOG	46
Table 3.5	Results from WFOG for Case 2	49
Table 3.6	Case 3: Previous studies: reported results and recomputed using WFOG	54
Table 3.7	Results from WFOG for Case 3	57

List of Figures

Figure 1.1	Power drop due to wakes at Horns Rev wind farm [after Mechali et al.]	7
Figure 2.1	Wind distribution for Case 3	13
Figure 2.2	Region for wind farm development and wind direction for Case 1	14
Figure 2.3	Cost of the wind farm vs. number of turbines, N_t	18
Figure 2.4	Rate of change of the cost function with N_t vs. N_t	18
Figure 2.5	Wake from a single wind turbine	20
Figure 2.6	Velocity recovery in the wake of a wind turbine. Non-dimensional velocity is shown against downstream distance, D , in rotor diameters from the wind turbine	22
Figure 2.7	Flowchart explaining the optimization process	27
Figure 3.1	Mosetti et al.'s optimal layout for Case 1 (after Mosetti et al.)	29
Figure 3.2	Grady et al.'s optimal layout for Case 1 (after Grady et al.)	29
Figure 3.3	Marmidis et al.'s optimal layout for Case 1 (after Marmidis et al.)	29
Figure 3.4	Optimal layout for Case 1 with coarse grid spacing using WFOG	33
Figure 3.5	Optimal layout when one column is optimized	35
Figure 3.6	Layout of the wind farm when one column is optimized	35

Figure 3.7	Optimal layout of the wind farm when all columns are optimized	35
Figure 3.8	Objective function values for different N_t for Case 1	39
Figure 3.9	Optimal layout for Case 1 with fine grid spacing using WFOG	39
Figure 3.10	Sub-optimal layout of the wind farm for Case 1 using WFOG (N44 b)	42
Figure 3.11	Sub-optimal layout of the wind farm for Case 1 using WFOG (N44 d)	42
Figure 3.12	Sub-optimal layout of the wind farm for Case 1 using WFOG (N44 e)	42
Figure 3.13	Mosetti et al.'s optimal layout for Case 2 (after Mosetti et al.)	46
Figure 3.14	Grady et al.'s optimal layout for Case 2 (after Grady et al.)	46
Figure 3.15	Objective function values for different N_t for Case 2	48
Figure 3.16	Optimal layout for Case 2 with fine grid spacing using WFOG	48
Figure 3.17	Wind distribution for Case 3	52
Figure 3.18	Mosetti et al.'s optimal layout for Case 3 (after Mosetti et al.)	54
Figure 3.19	Grady et al.'s optimal layout for Case 3 (after Grady et al.)	54
Figure 3.20	Objective function values for different N_t for Case 3	56
Figure 3.21	Optimal layout for Case 3 with fine grid spacing using WFOG	57

Nomenclature

N_t	Number of wind turbines
u	Velocity in the wake of a wind turbine
u_0, U_0	Free stream velocity
a	Axial induction factor
x	Downstream distance from the wind turbine
r_0	Rotor radius of the wind turbine
r_d	Wake radius at the downwind plane of the wind turbine
C_T	Thrust coefficient of the wind turbine
z	Hub height of the wind turbine
z_0	Surface roughness height of the site considered for the wind farm
r_1	Radius of the wake
η	Efficiency of the wind turbine
ρ	Air density
A	Area swept by the rotor of the wind turbine

Optimization of the Layout of Large Wind Farms

using a Genetic Algorithm

Abstract

by

ANSHUL MITTAL

In this study, a code ‘Wind Farm Optimization using a Genetic Algorithm’ (referred as WFOG) is developed in MATLAB for optimizing the placement of wind turbines in large wind farms to minimize the cost per unit power produced from the wind farm. A genetic algorithm is employed for the optimization. WFOG is validated using the results from previous studies. The grid spacing (distance between two nodes where a wind turbine can be placed) is reduced to $\frac{1}{40}$ wind turbine rotor diameter as compared to 5 rotor diameter in previous studies. Results are obtained for three different wind regimes: Constant wind speed and fixed wind direction, constant wind speed and variable wind direction, and variable wind speed and variable wind direction. Cost per unit power is reduced by 11.7 % for Case 1, 11.8 % for Case 2, and 15.9 % for Case 3 for results obtained using WFOG. The advantages/benefits of a refined grid spacing of $\frac{1}{40}$ rotor diameter (1 m) are evident and are discussed.

Chapter 1

Introduction

1.1. Overview

The wind is created by the earth's variations in temperature and air pressure. It is thus, a manifestation of solar energy, generated from large scale circulation when sun-heated air rises and cooler air sinks. It is estimated that about 2 percent of solar energy received by the earth is converted to the kinetic energy of the winds [1].

A wind turbine is a device which converts the wind's energy into electrical energy. This is achieved by blades, which are attached to a hub that rotates in response to the aerodynamic force of the wind on the blades. This rotation drives a generator which produces electricity that is transferred to the electrical power grid. A wind farm is a group of collocated wind turbines and may be thought of as a wind-driven power station. An advantage of a wind farm is that the fixed costs (management costs, electrical network related costs and project development costs) are spread over a bigger investment, thus, making wind energy competitive [2]. For a wind farm with 20 wind turbines; wind resource assessment is to be carried out for only one site and one installation is required to connect the wind farm to the electrical grid. Instead, if these 20 wind turbines are to be installed separately then, wind resource assessment for each site has to be conducted (i.e., 20 wind resource assessments) and 20 installations will be required to connect them to the grid which will make the electricity produced very costly as compared to the

electricity produced from the wind farm. The operation and maintenance of wind farms is easier and economical as all the wind turbines are in one location. However, the disadvantages associated with wind farms include power losses due to wakes of the wind turbines, increases maintenance of wind turbines due to increased turbulence in the wind farm.

The design of the wind farm involves several factors. These range from maximum desired installed capacity for the wind farm, site constraints, noise assessment for noise-sensitive dwellings, visual impact and the total cost. The fundamental aim, while designing a wind farm, is to maximize the power production while reducing the total costs associated with the wind farm. ‘Micro-siting’ is the process of optimizing the layout of the wind farm. This process is facilitated by the use of wind farm design tools (WFDTs) which are commercially available [3].

In this work, wind turbine placement in a wind farm is optimized using an objective function that represents the cost per unit power produced by the wind farm for a particular wind distribution function. The wind distribution function, in general, represents a model of wind variations in speed and direction averaged over a year, or many years. A genetic algorithm is employed for optimizing the placement of the wind turbines. An analytical wake model is utilized for modeling wind turbine wakes in the wind farm.

1.2. Wake Models

Wind turbine wakes have been studied for many years and various models have been developed by researchers. These models can be divided into two main categories, namely, analytical wake models and computational wake models. An analytical wake model characterizes the velocity in a wake by a set of analytical expressions whereas in computational wake models, fluid flow equations, whether simplified or not, must be solved to obtain the wake velocity field.

1.2.1. Analytical Wake Models

These are the simplest models. First introduced by Lanchester [4] and Betz [5], they are based on a control volume approach. Frandsen [6] developed a generalization of the Lanchester/Betz approximations and captured a family of previously developed wake models as well as advancing them to account for multiple interacting wakes. The model developed by Frandsen is limited in that it handles only regular array geometries i.e., the wind turbines should be in straight rows with equidistant spacing between turbines in each row and equidistant spacing between rows.

One of the most widely used wake model was developed by Jensen [7, 8]. He treated the wake behind the wind turbine as a turbulent wake which ignores the contribution of vortex shedding that is significant only in the near wake region. The wake model is, thus, derived by conserving momentum downstream of the wind turbine. The

velocity in the wake is given as a function of downstream distance from the turbine hub and it is assumed that the wake expands linearly downstream. Jensen also proposed that when two wakes interact, the resultant kinetic energy deficit¹ is equal to the sum of the kinetic energy deficits of the individual wakes at that point. So if the deficits in the two wakes are Δ_1 and Δ_2 the new resultant deficit, Δ_{12} , is their sum. The new velocity in the wake is just $U_\infty \left(1 - \sqrt{\Delta_{12}}\right)$. The same procedure applies to multiple interacting wakes.

Ishihara et al. [9] developed an analytical wake model by taking the effect of turbulence on the rate of recovery into account. They used a similarity approach to model the velocity profile (1.1 and 1.2) and defined wake recovery (parameter p) as a function of ambient turbulence and turbine generated turbulence. They calculated results for both offshore and onshore conditions and also at both high loading and low loading of wind turbine. These results compared well with experimental data obtained using a 1/100 scale model of Mitsubishi MWT-1000 wind turbine in a wind tunnel. The scale model used surface roughness models upstream of the wind turbine to simulate onshore conditions and a smooth upstream surface to simulate offshore conditions.

$$\frac{u}{U_0} = \frac{C_T^{\frac{1}{2}}}{32} \left(\frac{1.666}{k_1} \right)^2 \left(\frac{x}{2r_0} \right)^{-p} \exp \left(-\frac{r_0^2}{b^2} \right) \quad (1.1)$$

$$b = \frac{k_1 C_T^{\frac{1}{4}}}{0.833} d^{1-\frac{p}{2}} x^{\frac{p}{2}} \quad (1.2)$$

¹ The kinetic energy deficit at a point in the wake is the square of the difference between the free-stream velocity, U_∞ and the actual velocity at that point divided by free-stream velocity squared.

Werle [10] proposed a three part wake model: an exact model for the inviscid near-wake region, Prandtl's turbulent shear layer mixing solution for the intermediate wake and a far wake model based on the classical Prandtl / Swain axisymmetric wake analysis. No comparisons of the model with actual data have been published to date.

1.2.2. Computational Wake Models

Crasto et al. [11] modeled a single wake of a wind turbine using a CFD technique. He used RANS solver and $k-\epsilon$ turbulence model for closure. He compared the results of the simulation with wind tunnel data and reported over-estimating the velocity deficit in the far wake region after eight rotor diameters downstream of the wind turbine. He also compared the results with different analytical wake models. The Jensen and Ishihara models are in good agreement with Crasto's model for high thrust coefficient cases. However, the agreement is not so good for low thrust coefficient cases.

Crespo et al. [12] carried out an extensive survey of different modeling methods for wind turbine wakes. Apart from surveying various analytical wake models (discussed above) she reported the computational wake model UPMWAKE to be one of the best after comparing various models with wind tunnel measurements. In UPMWAKE, wind turbines are supposed to be immersed in a non-uniform basic flow corresponding to the surface layer of the atmospheric boundary layer. The properties of the non-uniform incident flow over the wind turbine are modeled by taking into account atmospheric stability, given by the Monin – Obukhov length, and the surface roughness. The

equations describing the flow are the conservation equations of mass, momentum, energy, turbulence kinetic energy and dissipation rate of turbulence kinetic energy. The modeling of the turbulent transport terms is based on the k- ϵ method for the closure of the turbulent flow equations.

Apart from the above discussed two categories of wake models, there is one other type of wake models where wind turbines are modeled as roughness elements [12, 13]. One of them was developed by Frandsen [13] where the drag from turbine and surface drag is combined to get the total drag. The limitation of these types of models is that the calculated total roughness is independent of wind direction and these models are best suited for predicting overall effects of large wind farms on wind characteristics.

1.3. Performance of Wake models compared to data from Wind farms

Researchers have analyzed the data available from operational wind farms and compared it with various wake models. Barthelmie et al. [14] analyzed the data measured using ship mounted SODAR and from three meteorological masts. The data was compared with various analytical and computational wake models to evaluate their performance. Barthelmie et al. concluded that performance of all the wake models is inconsistent and they either under-predict or over-predict the velocity deficit.

Data from Horns Rev wind farm (including the power output from selected wind turbines including some sited in wakes) was analyzed by Mechali et al. [15] to assess the

effect of wind direction relative to the row direction of the wind turbines. Horns Rev wind farm has 80 Vestas 2 MW wind turbines. The rotor diameter is 80 m with a hub height of 70 m. A large power drop (30 %) was observed from the windward turbine to the next turbine in it's wake when wind direction is in a narrow sector ($\pm 2^\circ$ along the row direction). The power drop from the first turbine to the second was as large as 50 % for wind coming from east (land fetch of about 15 km) as compared to wind coming from west (no land fetch) where power drop was only about 30 %. A slight recovery in the power produced from the wind turbines was also observed in the wind turbines towards the end of the row (See figure 1.1).

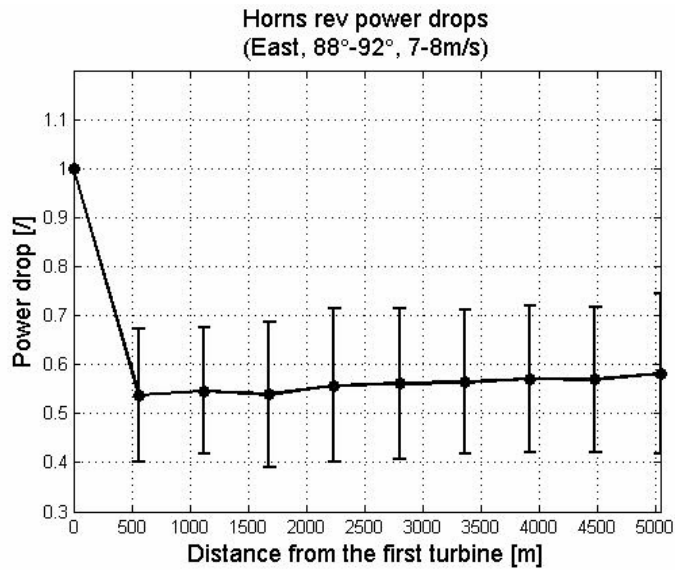


Figure 1.1 Power drop due to wakes at Horns Rev wind farm [After Mechali et al.]

Cleve et al. [16] analyzed 10 minute averaged data from the Nysted offshore wind farm for the period from September 2006 to March 2007. They attempted to fit the data to Jensen's analytical wake model (see above) by varying two parameters, namely, the wake decay factor (k or α) and the wind direction. Jensen's analytical wake model is

derived assuming static and homogenous wind conditions and as a result about two-thirds of the data was filtered out before the fitting process. The authors showed that the average value of the best fit wake decay parameter is 0.028; less than the current standard for offshore wake flows which is 0.04. This suggests that offshore wakes are narrower than was previously thought.

1.4. Optimization of turbine placement in a wind farm

Several researchers have utilized analytical wake models to optimize the placement of wind turbines in a wind farm. Use of computational wake models has been rare owing to high computational costs involved in obtaining specific results for each wind condition under consideration.

Beyer et al. [17] optimized three different wind farm configurations and compared them with expert guess configurations that were available for those wind farms. Expert guess configurations are mainly based on typical values for the averaged spatial density of the wind turbines: one wind turbine per three – four rotor diameter square area. Instead of using the wind distribution at the site under consideration, they simplified the analysis by using a single wind speed (the choice of wind speed was not justified by the authors).

Mosetti et al. [18] attempted to optimize the placement of wind turbines in a wind farm by employing a genetic algorithm. He used Jensen's analytical wake model for modeling the wakes of the wind turbines. His approach was to minimize the value of an

objective function which is weighted cost per unit power (though the actual values of the weights are not mentioned in the research paper). He obtained results for three scenarios

- Fixed wind direction at constant speed
- Variable wind direction but constant wind speed
- Variable wind direction with variable speed and some preferred directions

To implement the calculation, he used a coarse grid and set the distance between two adjacent nodes to be five wind turbine rotor diameters (in this case 200m). The results are discussed in Chapter 3 where they are compared to the results obtained in the present study.

Grady et al. [19] attempted the same problem as Mosetti et al. They examined the same three cases as Mosetti. Authors have used the exact same approach as was by Mosetti et al. such as Jensen's analytical wake model and a genetic algorithm for optimization. Grady et al. showed that Mosetti et al.'s results are not optimum. They suggested that the probable cause is that the solution was not allowed to evolve for sufficient generations (i.e., it was not converged to the optimum point).

Marmidis et al. [20] also attempted the same problem as Mosetti and Grady. The difference being that Marmidis et al. have analyzed only the simplest case in which wind comes from a fixed direction at a constant speed. Marmidis et al. used a Monte Carlo

method for optimizing instead of a genetic algorithm. No description of their method is given.

Elkinton et al. [21] attempted to minimize cost of energy. This is modeled as LPC (Levelized Production Cost) and includes investment cost, operation and maintenance cost and annuity factor. They have surveyed the available optimization algorithms, namely, Gradient search (GSA), Greedy heuristic (GHA), Genetic (GA), Simulated annealing (SAA), and Pattern search (PSA) algorithms. It is reported that GSA, GHA and PSA are fast but produce low quality results whereas, SAA and GA, though slow, produce high quality results. The authors tested GHA and GA by optimizing for four test cases and found that combination of GHA – GA performs either equal or better than GA. It is also reported that GHA alone gives highest LPC value thus, not good for optimization.

Elkinton et al. [22] developed a cost model for optimizing the layout of wind turbines in a wind farm. A genetic algorithm and greedy heuristic algorithm is used in series for optimization. Data from the Middlegrunden wind farm in Denmark is utilized for verification of the model. Jensen's analytical wake model is employed for modeling the wakes of the wind turbines. The cost model includes models for cost of rotor nacelle assembly, cost of support structure, electrical interconnection costs, operation and maintenance costs and decommissioning cost. When compared to data from Middlegrunden wind farm, large errors (~100%) in cost are reported and the error in the LPC (Levelized Production Cost which is the final objective function) is 29 %.

Acero et al. [23] attempted to maximize the power production by optimizing the placement of wind turbines in one dimension only. They have used Jensen's wake model and have varied hub height of wind turbines to improve the power production. GA and SAA are utilized for the optimization process.

In the present study, a method is developed using MATLAB for the three cases which Mosetti et al. and Grady et al. attempted. Results from earlier researches are used to validate the code. A refined grid (x200) is used in the present study. This will allow for more flexibility in placement of wind turbines. It also improves power production as wind turbines can be staggered so that wind turbines avoid the wakes of upstream wind turbines. Such staggered arrangements allow for more wind turbines to be placed in the same area while simultaneously increasing the efficiency of the wind farm and reducing the cost per unit power.

Chapter 2

Problem Description

2.1. Wind Regimes

The number of wind turbines and their placement is to be determined so that the cost per unit power for the entire wind farm is minimized. Three different cases representing three different wind regimes are considered.

Case 1. Constant Wind Speed and Fixed Wind Direction

This is the simplest case. The wind direction is fixed the speed is constant at 12 m/s.

Case 2. Constant Wind Speed and Variable Wind Direction

The wind direction is variable and the speed is constant at 12 m/s. There is an equal probability that the wind blows from any direction. The wind direction is discretized in 36 segments each measuring 10° .

Case 3. Variable Wind Speed and Variable Wind Direction

Here both the wind speed and the direction are variable. Figure 2.1 shows the wind distribution. Three wind speeds are possible, 17, 12 and 8 m/s. The probability of the wind speeds is higher from wind directions between 270° to 350° .

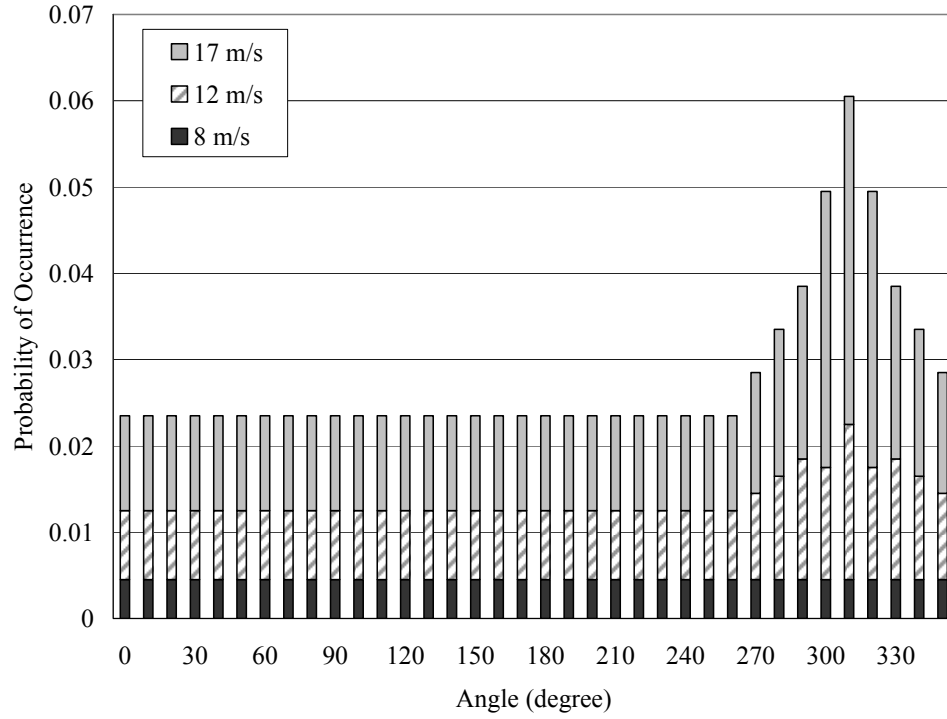


Figure 2.1 Wind distribution for Case 3

2.2. Factors in Wind Farm Design and Assumptions

The process of designing a wind farm is a complicated process with numerous constraints affecting the design. The first factor in wind farm development is land availability which determines how much space is available for the wind farm. For the purpose of this study, a 2 km by 2 km square region is considered and is shown in figure 2.2. It is assumed that region is flat with a surface roughness height of 0.3 m which is characteristic of a land or onshore site.

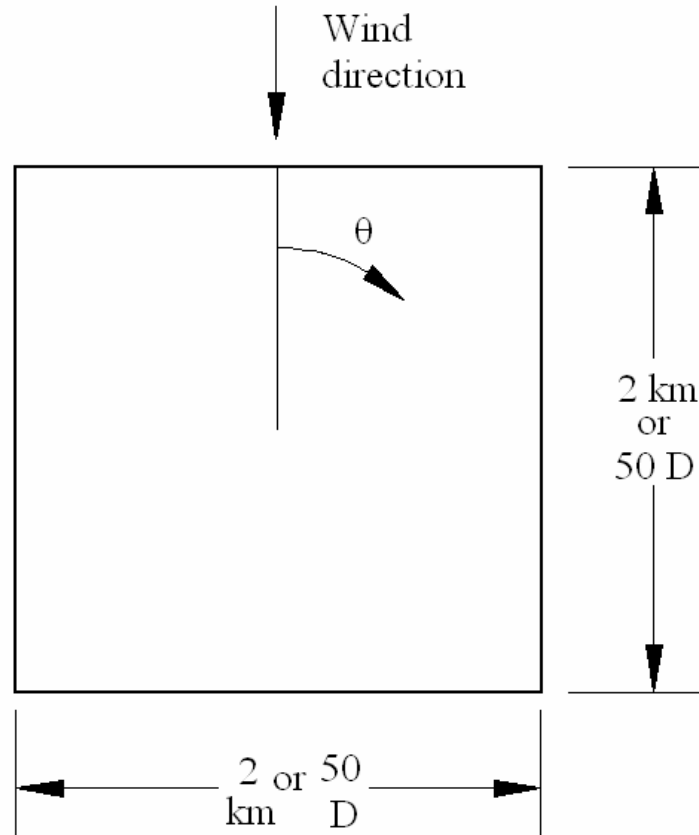


Figure 2.2 Region for wind farm development and wind direction for Case 1

Other important constraints are the maximum installed capacity and the total cost of the wind farm. The maximum installed capacity is the maximum amount of power that the wind farm would produce and is generally determined by available connections to the electrical grid and terms of the power purchase agreement. The total cost of the wind farm is governed by the amount of capital available for wind farm development. In the present study, these two factors are not considered. This means that there is no limit on the amount of the power produced and on the total cost of the wind farm. Note that, the objective of the study is to minimize the cost per unit power for the wind farm. By having no limits on the power produced and the total cost, the complete design space can be

explored and an optimal design can be obtained with land being the only limiting parameter.

Other factors include the affect of the noise from the wind farm on the noise-sensitive dwellings near-by and the visual impact of the wind farm. As these factors are specific to each site, they are not considered in the present study.

Figure 2.2 shows the wind direction for Case 1 and specifies clockwise measurement of angle for Cases 2 and 3. The reference angular measurement direction is not specified in any of the previous studies which could create confusion and ambiguity in Case 3. The results for Case 2 are not affected by this. This issue is discussed in detail in the Chapter 3.

The wind turbines are assumed to have a rotor diameter of 40 m and a hub height of 60 m. The thrust coefficient of the wind turbine is assumed to be constant at 0.88. Only one type of wind turbine is used in the wind farm and modeling the effects of different types of wind turbines or same wind turbine with different hub heights (or the same turbines on variable terrain) is not within the scope of this work.

A 100 m deep space (2.5 rotor diameters) is “off-limits” to wind turbines along the perimeter of the 2 km by 2km region. This is done because to leave some buffer space in case a wind turbine is placed on the edge of the 2 km \times 2 km region during optimization process. By leaving this border/buffer space, results from present study can

be compared accurately and without any confusion to results from previous studies [18, 19, 20].

The closer the turbines are spaced, higher the velocity deficit associated with the upwind turbine. This leads to a reduction in power output of the downwind turbine. This in turn decreases the total power produced by the wind farm. Thus, too close a spacing will increase the cost per unit power. For situations where the wind is unidirectional (artificial), or there is a 360° wind distribution with a dominant wind direction or directions, the turbine spacing perpendicular to the dominant direction must also be accounted for, even though no turbine is affected by the other's velocity deficit when the wind blows from that direction. Thus, in WFOG, a minimum distance of 200 m (corresponding to five wind turbine rotor diameters) is set between any two turbines. If any wind turbine is less than 200 m from any other wind turbine, then WFOG treats that wind turbine as if it is not operational and no power is being produced. In other words, close proximity layouts will not be optimum and would anyway get rejected in the optimization process.

To optimize the cost per unit power (objective function) for a wind farm, the total cost of the wind farm is to be determined and the total power produced is to be calculated.

$$\text{Objective function} = \frac{\text{Cost}}{\text{Total Power}} \quad (2.1)$$

2.3. Cost Model

To determine the cost of the wind farm, a cost model is selected. The model chosen was also used in previous studies [18, 19, 20]. The total cost is only dependent on the number of wind turbines installed in the wind farm. This model gives the non-dimensional cost of the wind farm as a function of the number of wind turbines and is based on that some discount is available when large number of wind turbines is purchased. Thus, a maximum reduction in cost of 1/3 is possible when very large number of wind turbines is purchased. The total cost of the wind farm is

$$Cost = N_t \left[\frac{2}{3} + \frac{1}{3} e^{-0.00174 N_t^2} \right] \quad (2.2)$$

where, N_t is the number of wind turbines purchased.

Figure 2.3 shows the total cost plotted against N_t . The first derivative of the cost function is also plotted in figure 2.4 against the number of wind turbines. An important point that comes out is the first derivative of the cost function has a minima between $N_t = 29$ and $N_t = 30$ and increases monotonically for $N_t > 30$. This implies that the cost of the $(N+1)^{th}$ turbine is more than the cost of the N^{th} turbine for $N > 30$. For example, the cost of the 32nd wind turbine is 0.521, slightly less than the cost of the 33rd wind turbine which is 0.525. The significance of the first derivative is discussed in Chapter 3 (Section 3.1.2.)

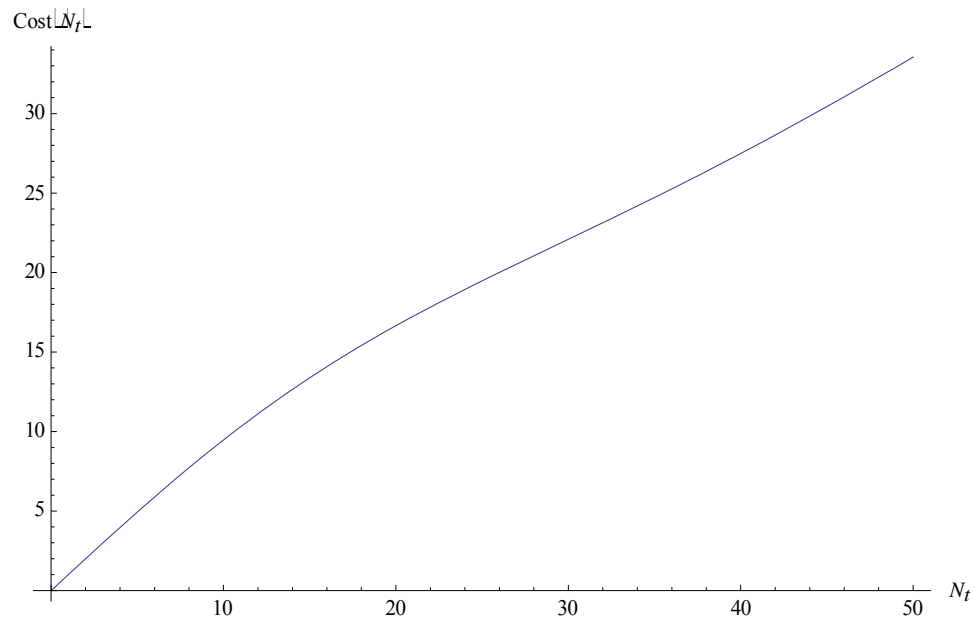


Figure 2.3 Cost of the wind farm vs. number of turbines, N_t

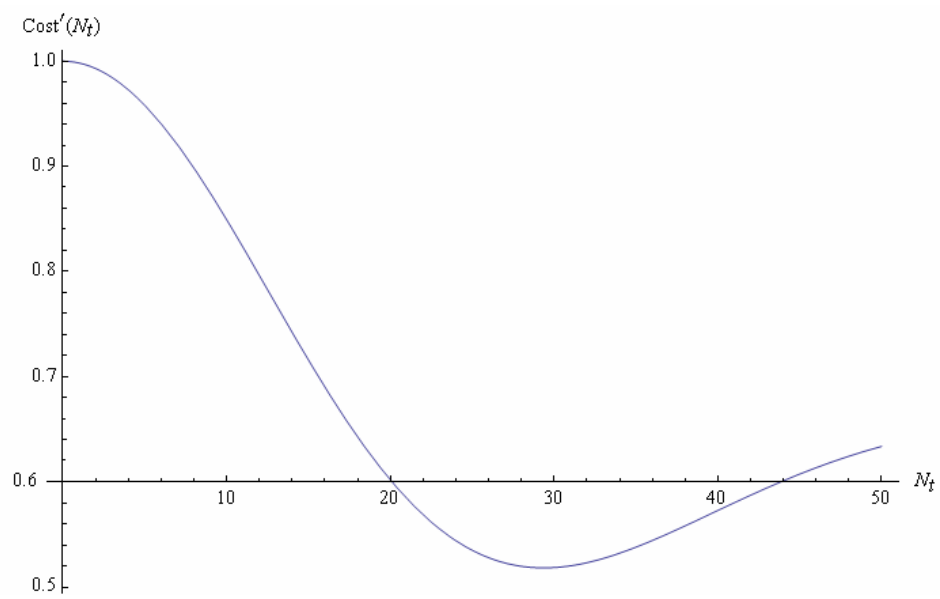


Figure 2.4 Rate of change of the cost function with N_t vs. N_t

For calculating the power produced from the wind farm, wake losses due to wakes of the upstream wind turbines must be taken into account. There are several possible ways to do this (see Chapter 1). For this study, an analytical wake model developed by Jensen [7, 8] is chosen. The model gives an expression for determining the velocity in a wake as a function of downstream distance. The wake model is discussed in detail in the next section.

2.4. The Jensen's Wake Model

To estimate the power produced from a wind turbine operating in the wake of one or more wind turbines, an analytical wake model developed by Jensen [7, 8] is chosen. It is based on global momentum conservation in the wake downstream of the wind turbine. This model is based on the assumption that the wake is turbulent and the contribution of tip vortices is neglected. This means this wake model is strictly applicable only in the far wake region [7, 8]. Jensen also assumed that the wake expands linearly with downstream distance as shown in figure 2.5. Refer to Appendix B for the derivation of the Jensen's wake model.

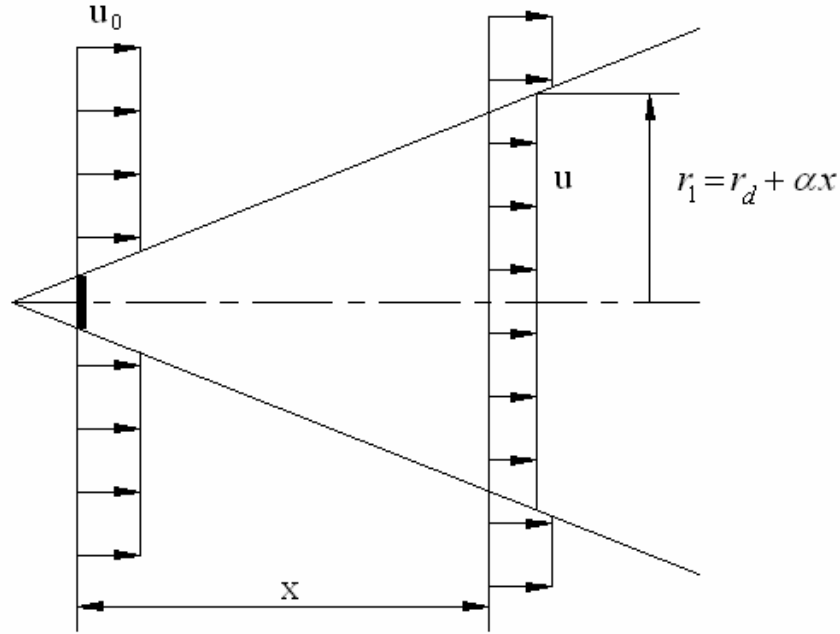


Figure 2.5 Wake from a single wind turbine

The velocity, u , in the wake at downstream distance, x , from the wind turbine is given by

$$u = u_0 \left[1 - 2a \left(1 + \frac{\alpha x}{r_d} \right)^{-2} \right] \quad (2.3)$$

where, u_0 , is the wind velocity unaffected from any wind turbine or free stream velocity.

a , is the axial induction factor and is calculated from the thrust coefficient, C_T , of the wind turbine. As the wind approaches the wind turbine, it slows down. The ratio of this reduction and the free stream velocity is called the axial induction factor. The value of a should be less than 0.5.

$$C_T = 4a(1-a) \quad (2.4)$$

The wake radius immediately upstream of the wind turbine is equal to the wind turbine rotor radius but as the energy is extracted from the wind across the width of the blade, the wake expands. The wake radius immediately downstream of the wind turbine is called downstream rotor radius of the wind turbine, r_d , and is computed using

$$r_d = r_0 \sqrt{\frac{1-a}{1-2a}} \quad (2.5)$$

α is called entrainment constant [7] and signifies how fast or slow wake expands. It is calculated using an empirical expression

$$\alpha = \frac{0.5}{\log\left(\frac{z}{z_0}\right)} \quad (2.6)$$

Here, z_0 is the surface roughness height of the site, which is 0.3 m for the site considered in the present study and z is the hub height of the wind turbine, 60 m for the wind turbine under consideration.

The radius of the wake at any distance, x , downstream of the wind turbine is

$$r_1 = r_d + \alpha x \quad (2.7)$$

Figure 2.6 shows the plot of the velocity in the wake of a wind turbine as a function of the downstream distance. It is seen that at 10 rotor diameters downstream of the wind turbine (corresponding to 400 m), velocity is only 88.2 % of the free-stream velocity. Thus, at 10 D downstream, 11.8 % of the free-stream velocity is not available which translates into a power loss of 31.3 % due to the wake of the upstream wind turbine.

For cases where a wind turbine encounters multiple wakes from numerous upstream wind turbines, the Jensen model is extended as follows. The resultant velocity in the merged wake is calculated by equating the kinetic energy deficit of the merged wake to the sum of the kinetic energy deficits of the individual wakes at that point.

$$\left(1 - \frac{u}{U_0}\right)^2 = \sum_{i=1}^{N_t} \left(1 - \frac{u_i}{U_0}\right)^2 \quad (2.8)$$

Thus, to calculate the cost per unit power for any wind farm, the cost of the wind farm is determined which in this case is only dependent on the number of wind turbines (see equation (2.2)) and the power produced from the wind farm which is dependent on the number of wind turbines and their placement.

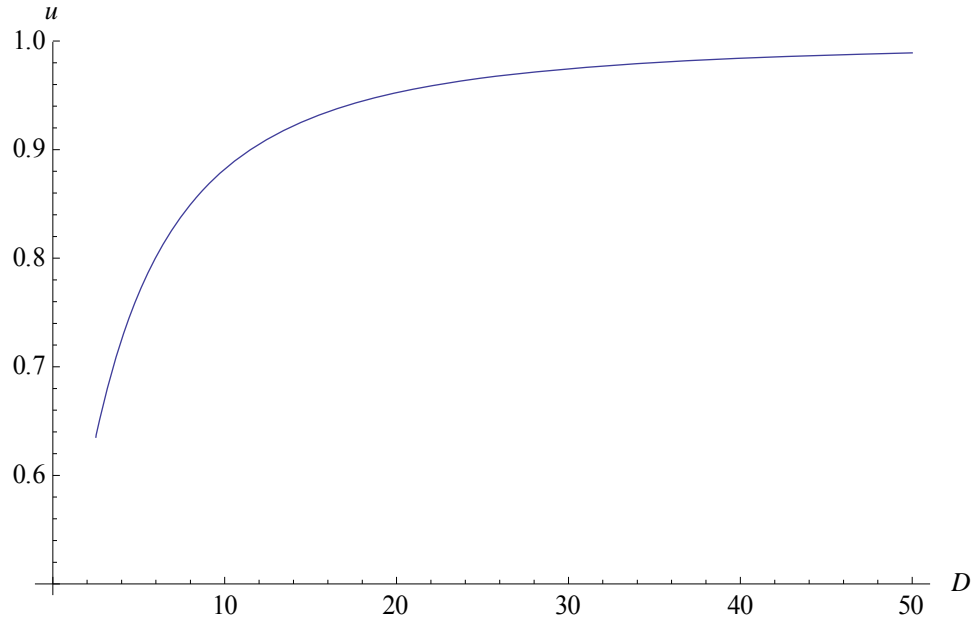


Figure 2.6 Velocity recovery in the wake of a wind turbine. Non-dimensional velocity is shown against downstream distance, D, in rotor diameters from the wind turbine

2.5. Power Calculation

WFOG analyzes layouts of wind farm sent from the ‘ga’ solver. It receives the coordinates (x and y) of each wind turbine in the layout, calculates power produced from it and adds it up to get the total power produced from the wind farm.

For a wind turbine, available power in wind is given by,

$$\text{Available power} = \frac{1}{2} \rho A u^3 \quad (2.9)$$

The power produced from a wind turbine is.

$$\text{Power produced} = \eta \frac{1}{2} \rho A u^3 \quad (2.10)$$

Assuming wind turbine efficiency, η , to be 40 %, power produced from the wind turbine considered in this study is,

$$\text{Power produced} = \frac{40}{100} \times \frac{1}{2} \times 1.2 \times \pi \times (20)^2 \times u^3 \quad (2.11)$$

$$\text{Power produced} = 301 \times u^3 \text{ W} = 0.3 u^3 \text{ kW} \quad (2.12)$$

To calculate the power produced from a wind turbine, it is checked whether the wind turbine under consideration is operating in the wake of any other wind turbine. If this is not the case, then power is calculated using the free stream velocity, otherwise wind velocity at the point where concerned wind turbine is placed is determined using the analytical wake model discussed earlier.

2.6. Optimization Process

A code is developed in MATLAB (referred to as WFOG) which calculates the power produced and the cost of a wind farm. WFOG is coupled with the genetic algorithm solver, 'ga' solver, available in MATLAB's genetic algorithm toolbox for optimization process. This toolbox has two genetic algorithm solvers. The 'ga' solver is a genetic algorithm solver for single objective functions. A second solver is 'gamultiobj' which is also a genetic algorithm solver but is used for optimization of multiple objective functions.

2.6.1. Initialization

The flowchart in figure 2.7 explains the process through which WFOG and 'ga' solver operate to find an optimal solution. The optimization process starts with the initialization in the genetic algorithm 'ga' solver. In the initialization process, following parameters are specified.

- a. Number of variables: A solution is a layout of the wind farm with a defined number of wind turbines. The number of variables is twice the number of wind turbines because two variables are required to specify the position of a wind turbine in a two dimensional region.
- b. Population size: The population size is the total number of solutions in one solution set (population).

- c. Constraints: The constraints in the ‘ga’ solver are specified as bounds i.e., lower and upper limits for the variables. The size of the wind farm is specified in constraints so that wind turbines can not be placed outside the wind farm region.
- d. Optimization criteria: The optimization criteria include maximum number of iterations (referred as generations), stall generations (i.e., if average change in objective function value over stall generations is less than function tolerance than algorithm stops) and function tolerance. The optimization criteria are referred to as stopping criteria in the ‘ga’ solver.

2.6.2. The Genetic Algorithm Solver or ‘ga’ solver

After the initialization process, random set of solutions is created taking into account the constraints. All the solutions created are analyzed by WFOG. Estimated power production and the cost of the wind farm are calculated in WFOG and objective function value (cost per unit power) of each solution is returned to ‘ga’ solver.

In the next step optimization criteria are checked if they are satisfied or not. When the optimization criteria are not met, all the solutions are ranked based on their objective function values. A solution with small objective function value is better as its cost per unit power is smaller and is placed before other solutions with larger objective function value. For example, a solution with objective function value of 0.02 is placed before a solution with objective function value of 0.03.

After ranking is completed, some solutions are selected based on which new solutions are created (reproduced). This selection of solutions is affected by the ranking done in previous step and a solution with good ranking has a better chance of being selected. New solutions are created but some solutions are copied from original set of solutions to the new set of solutions. These selected few solutions are one of the best in terms of the ranking and are called elite count.

The last step before new set of solutions (new population) is ready is called Mutation. In this step some random changes are made in few solutions. This step is very important as it helps in maintaining diversity in the solution set. This new solution set is analyzed by WFOG and this iterative procedure continues until one of the optimization criteria is satisfied.

2.6.3. Post-processing

Once the computations have stopped, the results are exported from the ‘ga’ solver and the exported structure is saved to a file for later use. The coordinates of all the wind turbines are saved in a separate variable and analyzed by WFOG to determine the power produced. The layout can be plotted as per the requirement.

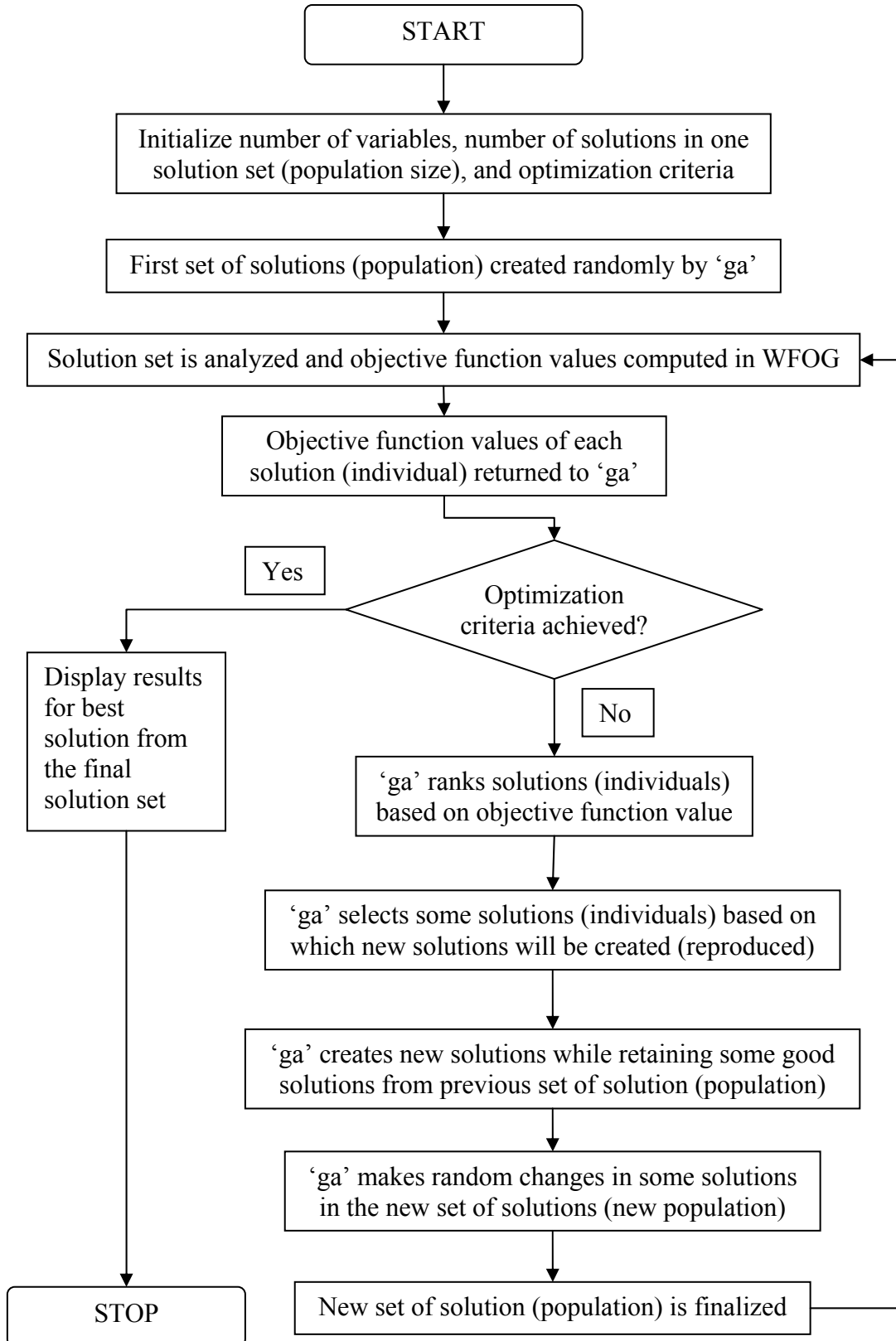


Figure 2.7 Flowchart explaining the optimization process

Chapter 3

Results and Discussion

In this chapter, results obtained using the model described in chapter 2 are presented and compared to the results from previous studies [18, 19, 20]. Results are obtained for three cases: Constant wind speed and fixed wind direction, constant wind speed and variable wind direction, and variable wind speed and variable wind direction. In each case, the number of turbines, N_t , is specified and the optimal configuration for N_t is obtained by minimizing the objective function (2.1). The minimum value of the objective function is then compared across a range of N_t to obtain the optimal number of wind turbines to be placed in the wind farm for each case.

3.1 Case 1: Constant Wind Speed and Fixed Wind Direction

3.1.1 Results from previous studies

This case was attempted by Mosetti et al. [18], Grady et al. [19], and Marmidis et al. [20] using a coarse grid with five wind turbine rotor diameters (200 m) as the distance between adjacent grid points. A wind turbine can be placed at a grid point which means minimum distance between any two turbines can be 200 m. The optimal layouts and results from these studies are presented in Figures 3.1 – 3.3 and Table 3.1. The optimal configurations from previous studies were recomputed using WFOG and results are presented alongside the reported results in Table 3.1. Note that the efficiency presented in results is the efficiency of the wind farm and should not be confused with the efficiency

of the wind turbine. It represents the actual power produced from the wind farm compared to the power produced from the same number of turbines experiencing the free-stream wind speed (i.e., no wake losses in the wind farm).

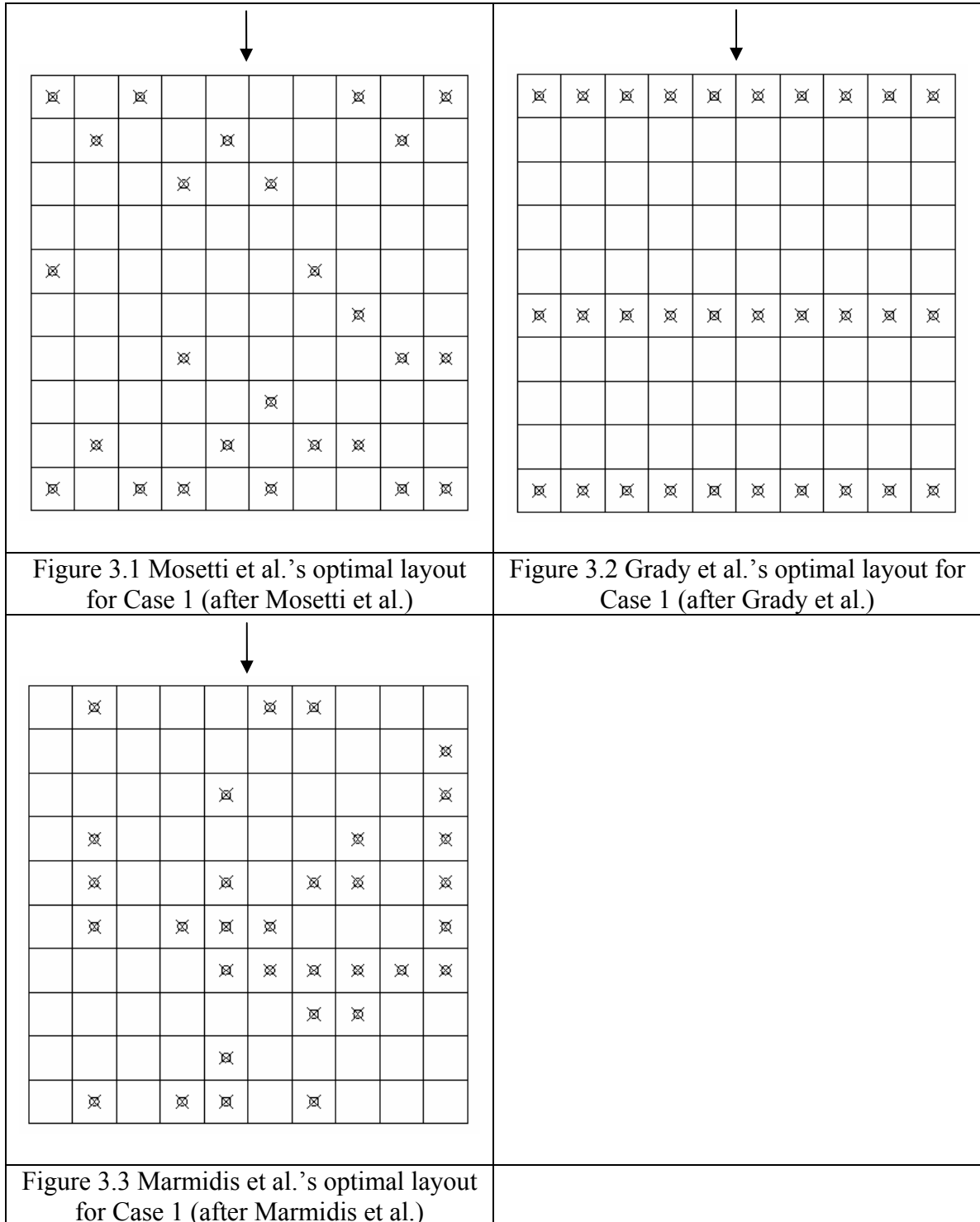


Table 3.1 Case 1: Previous studies: reported results and recomputed using WFOG

	Mosetti et al.		Grady et al.	
	Reported	WFOG	Reported	WFOG
Number of Turbines	26	26	30	30
Total Power (kW)	12352	12369	14310	14336
Objective function value (1/kW)	1.6197×10^{-3}	1.6175×10^{-3}	1.5436×10^{-3}	1.5408×10^{-3}
Efficiency (%)	91.645	91.769	92.015	92.181
	Marmidis et al.			
	Reported	WFOG		
Number of Turbines	32	32		
Total Power (kW)	16395 ²	11435		
Objective function value (1/kW)	1.4107×10^{-3}	2.0227×10^{-3}		
Efficiency (%)	Not Reported	68.932		

² See discussion on page 30

The layout reported by Mosetti et al. is not symmetrical. This is, in spite of the fact, that wind is unidirectional and has a fixed speed. This means that the wind conditions are same for all the columns. The first wind turbine in any column is placed in the first three rows except for column seven in where the first turbine appears in row five. Similarly, last wind turbine in all the columns is placed in last two rows.

The results reported by Grady et al. are symmetrical because he optimized only one column and translated the results to all the columns. The symmetrical configuration has an objective function value lower than that of Mosetti et al. Thus, it can be said that Mosetti et al. were not able to reach the optimal solution but were close because the pattern in layout reported by Grady et al. can be seen in Mosetti et al.'s layout.

Figure 3.3 shows the layout presented by Marmidis et al. and it is questionable because there are no wind turbines in column one and three. This means these two columns are not utilized as the wind direction is along the column. Moreover, in column ten, six wind turbines are placed back to back which will severely affect the efficiency and power production from these wind turbines.

The results of the WFOG computations are in agreement with those reported by Mosetti and Grady but there is a discrepancy in the power output and objective function value reported by Marmidis et al. This discrepancy is further investigated by modifying the reported layout as follows. Two wind turbines are moved from their existing positions

to new positions and power output from the modified wind farm is calculated. Wind turbine at row 3, column 10 location is moved to row 1, column 1 location and wind turbine at row 5, column 10 is moved to row 1, column 3 location. The estimated power output from the modified wind farm is calculated to be 12245 kW with an objective function value of 1.8888×10^{-3} . This shows that the layout reported by Marmidis et al. cannot be optimum because a modified version of the reported layout produces more power with the same number of wind turbines.

At this point it is clear that the WFOG calculations are consistent as results from two of the three studies referred to earlier agree very well with the WFOG computations while in the third case, the reason for the disagreement is readily explained. It is also shown that for a unidirectional fixed wind speed case, the optimal layout is symmetrical with wind turbines placed as far away from each other as possible (only along the wind direction) to minimize the wake losses.

3.1.2 Results from WFOG with coarse grid spacing

In the previous section (3.1.1), WFOG was used to check for consistency of results reported in previous studies. In this section, WFOG was used for optimization, with all the parameters the same as in previous studies. This was done to test whether the results reported in earlier studies [18, 19] are optimal and if not, then WFOG was used to find the optimal solution. For this purpose, the distance between two adjacent nodes (grid points) was set to 200 m (as in the previous studies) in WFOG.

WFOG minimizes the objective function (cost per unit power) using a coarse grid spacing (200 m). The optimal layout, as presented in figure 3.4, is same as obtained by Grady et al. However, an important point to note is that Grady et al. assumed that, since the wind is unidirectional it was sufficient to optimize only one column (i.e., a one dimensional solution) and translate the result to all other columns. His reasoning was that, for the typical grid spacing, wind turbine and the wake model under consideration, the wakes from wind turbines in adjacent columns do not interact and, thus, wind turbines in one column do not affect power output of wind turbines in adjacent columns.

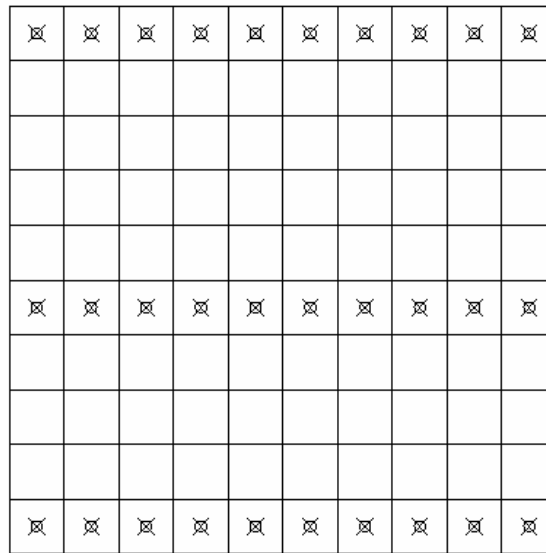
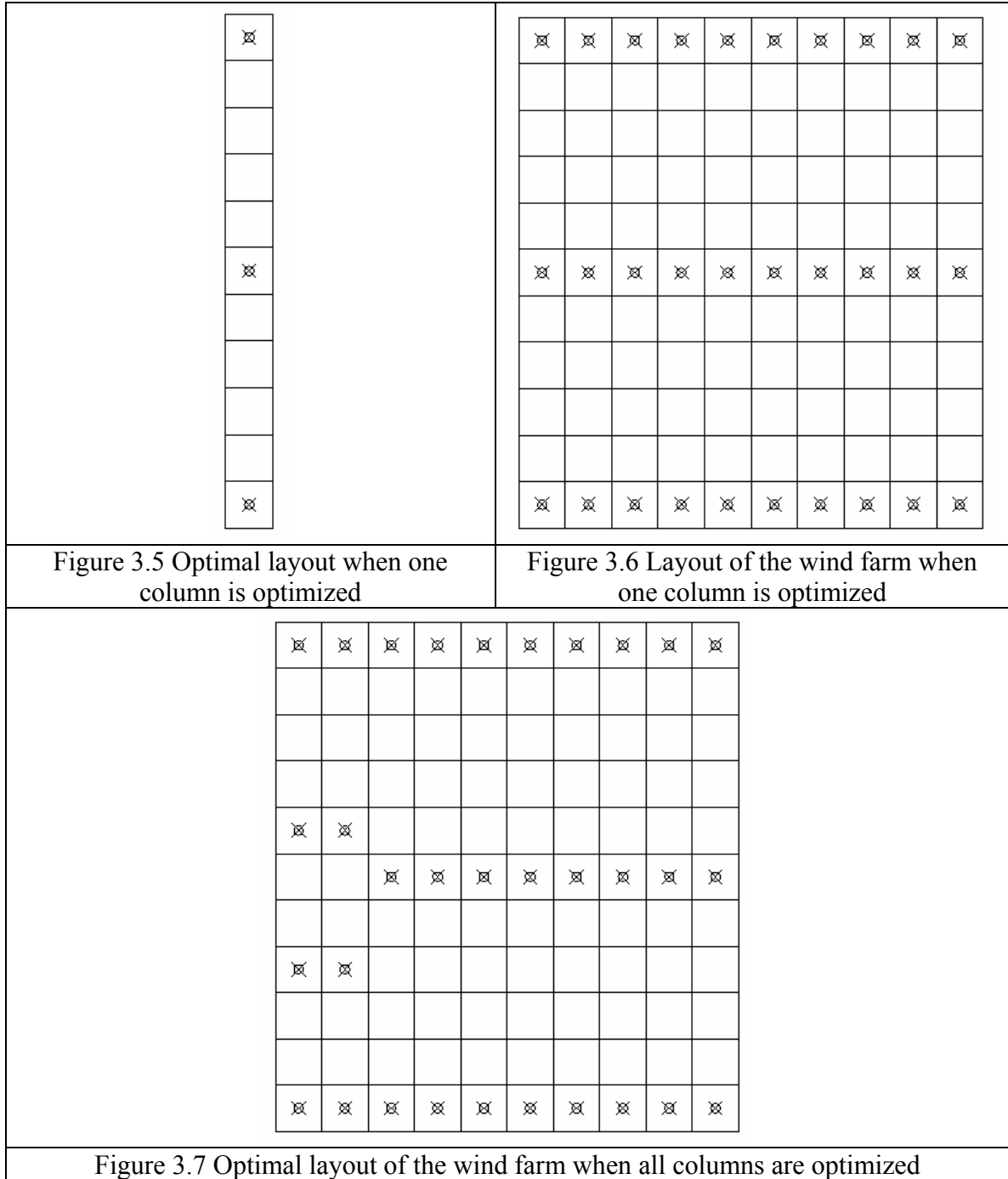


Figure 3.4 Optimal layout for Case 1 with coarse grid spacing using WFOG

However, it was found that, even though wind turbines in adjacent columns operate independently of each other, the result need not be one dimensional. The underlying reason is that the cost function is nonlinear in N_t , the number of wind turbines

and the result obtained for a single column may not necessarily be optimum for multiple columns.

To illustrate this point, two separate calculations are undertaken. A wind farm region is considered which is 2 km wide (same as the previous studies) and 2.2 km long (2 km in the previous studies). As in the previous case, there are 10 columns but there are 11 rows. In the first calculation only one column is optimized and the solution is as shown in figure 3.5 with three wind turbines. On translating this solution over all the columns, the layout of the wind farm will be as shown in figure 3.6. This wind farm will produce 14530 kW power at a cost per unit power (objective function value) of 1.5202×10^{-3} .



However, if a two dimensional solution is obtained (second calculation), i.e., all ten columns are considered for optimization simultaneously, the optimal solution consists of 32 wind turbines as shown in figure 3.7. This wind farm will produce 15218 kW at a

cost per unit power of 1.5198×10^{-3} . Figure 3.7 shows that the first two columns have four wind turbines and the remaining columns have three wind turbines. This solution is not unique in terms that position of columns can be interchanged without affecting the cost per unit power of the wind farm. The explanation for this is that the wakes of wind turbines in one column do not affect wind turbines in adjacent columns.

When 30 wind turbines are placed, the total cost of these wind turbines is 22.088 and they produce 14530 kW power. When two additional wind turbines are added and the layout is modified (see figure 3.7), these two additional wind turbines produce 688.2 kW power and their cost is 1.04019 which means the cost per unit power of the power produced from these two additional wind turbines is 1.5114×10^{-3} which is less than the cost per unit power of the power being produced by earlier 30 wind turbines (1.5202×10^{-3}). But if one more wind turbine is added (i.e., 33rd wind turbine), the additional power produced is 344.1 kW and the cost of this wind turbine is 0.525. This means the cost per unit power for the 33rd wind turbine is 1.5257×10^{-3} . The reason why 33rd wind turbine, in spite of producing the same amount of power as 32nd wind turbine does not reduce the cost per unit power for the wind farm, is because the first derivative of the cost function with respect to the number of wind turbines, N_t , increases continuously for $N_t > 30$ (see figure 2.4 in chapter 2). In other terms, the cost of 33rd wind turbine (0.525) is more than the cost of the 32nd wind turbine (0.521).

The results reported by Grady et al. are optimal and it is also found that the solution is two dimensional. This is in spite of the fact that power production from each

column is independent of all the other columns. Moreover, it can be concluded that WFOG is consistent and works well when coupled with the ‘ga’.

3.1.3 Results from WFOG with fine grid spacing

In this section, results from WFOG with a fine grid spacing are presented. The spacing between two adjacent grid points, where a wind turbine can be placed, is adjusted to 1 m. This allows for more flexibility in placing the wind turbines in the wind farm. Optimization is carried out using the refined grid spacing for different number of wind turbines as number of wind turbines, N_t , is also a variable. For each N_t (i.e., number of wind turbines), the ‘ga’ solver is run several times and several optimal solutions are obtained.

The graph in figure 3.8 shows the objective function value on the y axis and number of wind turbines on the x axis. The objective function value plotted is the minimum value obtained out of the several runs for each number of wind turbines. The graph shows that as N_t is increased, cost per unit power for the wind farm reduces, thus, meaning that installing more wind turbines in the wind farm is economical. This trend is evident till N_t reaches the value of 44 after which objective function value (cost per unit power) starts to increase slowly with N_t . The lowest cost per unit power is 1.3602×10^{-3} for 44 wind turbines. The optimal layout of these 44 wind turbines is shown in figure 3.9.

The optimal layout of 44 wind turbines produces 21936 kW (see Table 3.2). A unique pattern is evident in the layout (Figure 3.9) in which wind turbines, in groups of

three or four, are placed in straight lines which are at an angle to the wind direction. The reason is that any wind turbine, which is to be placed downstream of a wind turbine, is placed in a way so that it is outside the wake of the upstream wind turbine. Thus, wind turbines get placed in such a way that each wind turbine placed downstream avoids the wakes of all the upstream wind turbines. The wake of a wind turbine is shown as hatched area in figure 3.9. Please note that the two immediate downstream wind turbines are not in the wake.

For the coarse grid spacing used in previous calculations, the optimal number of wind turbines was 30. Thus, it is clear that due to more flexibility in placing wind turbines by using a refined grid spacing of 1 m, not only can more wind turbines be placed in a given space but they can be placed in a way so that they operate at higher efficiency. In this case, 14 more wind turbines can be placed in the wind farm (30 wind turbines in coarse grid spacing calculations and 44 wind turbines in fine grid spacing calculations) and the wind farm operates at an increased efficiency of 96.1 % as compared to 92.1 % in case of coarse grid spacing calculations.

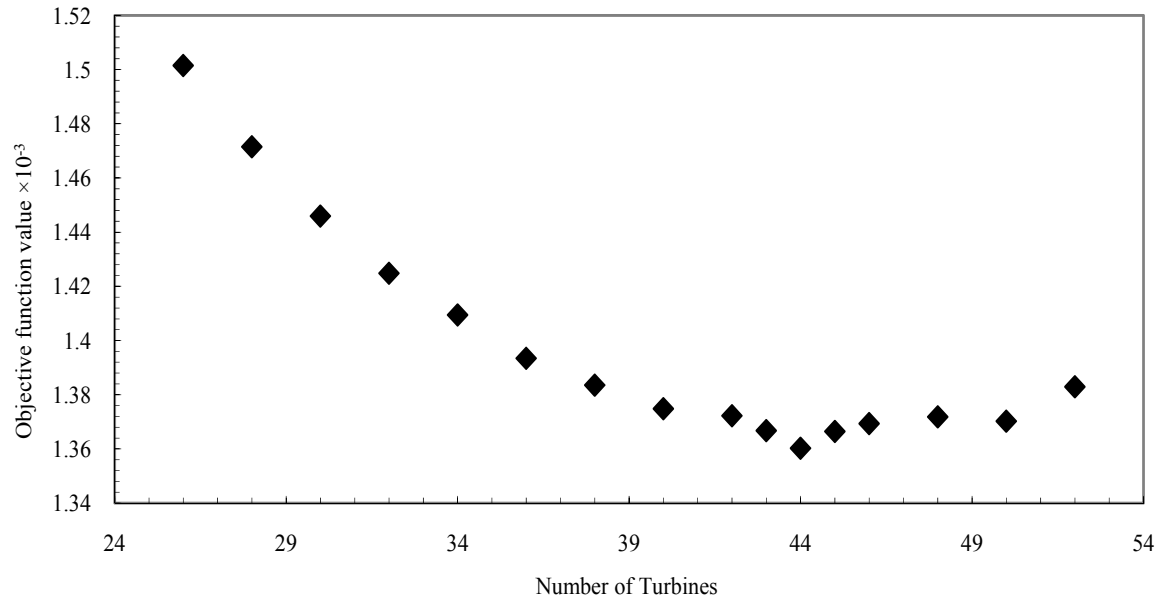


Figure 3.8 Objective function values for different N_t for Case 1

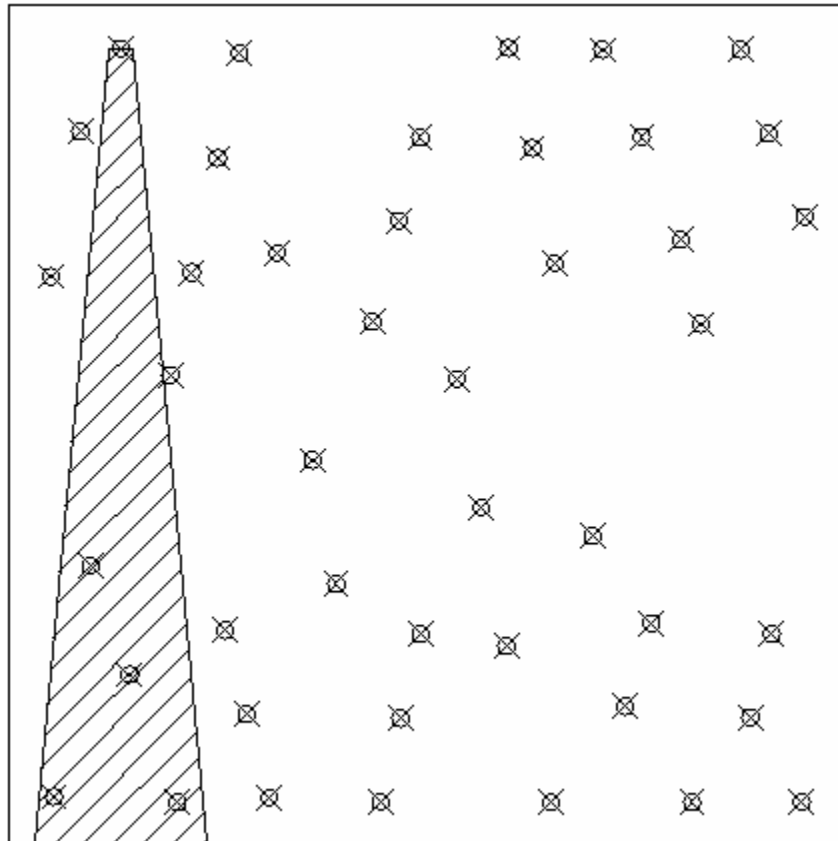


Figure 3.9 Optimal layout for Case 1 with fine grid spacing using WFOG

Table 3.2 Results for optimal layout from WFOG for Case 1

	WFOG (1 m grid spacing)
Number of Turbines	44
Total Power (kW)	21936
Objective function value (1/kW)	1.3602×10^{-3}
Efficiency (%)	96.170

As stated earlier in this section, the ‘ga’ solver was run several times for each N_t . The results obtained in each run are close to the solution presented earlier in figure 3.9. Some of these close to optimal layouts are presented in figures 3.10 – 3.12. Table 3.3 gives the objective function values, estimated power production and efficiency of these layouts. The significance is that the solution to this problem (the spatial arrangement of the wind turbines) is not unique, in that there are several arrangements of the same number of turbines that will produce almost the same amount of power. This will be an advantage in cases where it is not possible to install wind turbines in a particular area due to imposed or natural site constraints, etc.

In all the layouts (Figures 3.10 – 3.12), the unique pattern discussed earlier is visible. Moreover, in all the layouts, including layout in figure 3.9, the same pattern is observed and some regions in the middle part of the wind farm are not used for placing wind turbines. This is clearly evident in figure 3.12, in which a large region on the left side of the wind farm does not have any wind turbines. A possible explanation for this is discussed below. The wakes of all the wind turbines in the groups placed in the top region of the wind farm recover at a fixed rate. If wind turbines, in general, are placed in the middle part of the wind farm, then these wind turbines will not be able to avoid these wakes (because wakes expand downstream even as they recover) and will, thus, produce less power. However, if instead of placing turbines in the middle of the wind farm, these wind turbines, in groups, are placed in the bottom part of the wind farm, the wakes would have recovered and wind turbines will not suffer from wake losses. For example, the velocity in the wake of a wind turbine at 800 m downstream is 95.2 % of the free stream velocity as compared to 98.4 % at 1600 m downstream of the wind turbine (see figure 2.6). This translates to that if a wind turbine is placed in the wake at 800 m downstream, then it will produce 86.4 % power as compared to a wind turbine placed outside any wakes. If the downstream distance is increased from 800 m to 1600 m, then, the power production increases from 86.4 % to 95.3 %.

The WFOG results with fine grid spacing are better than those reported by Grady et al. The advantages of utilizing fine grid spacing become evident as more wind turbines are placed in the same space and the overall efficiency of the wind farm has also increased by 4 %.

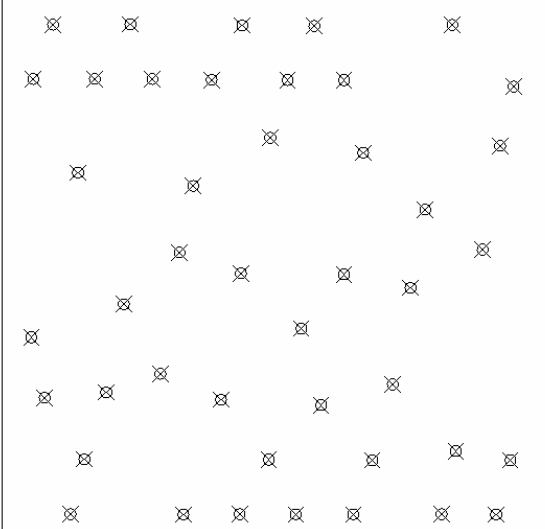
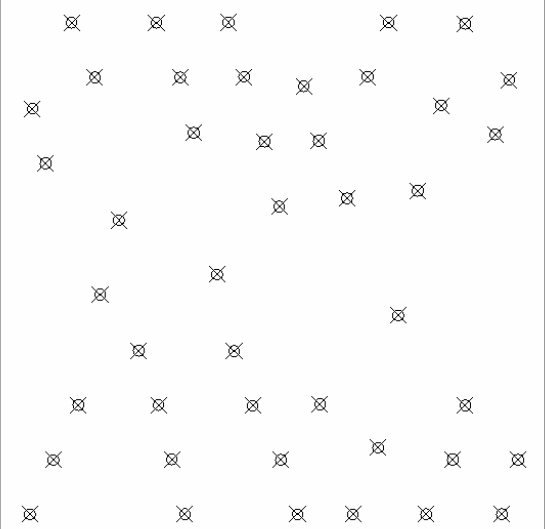
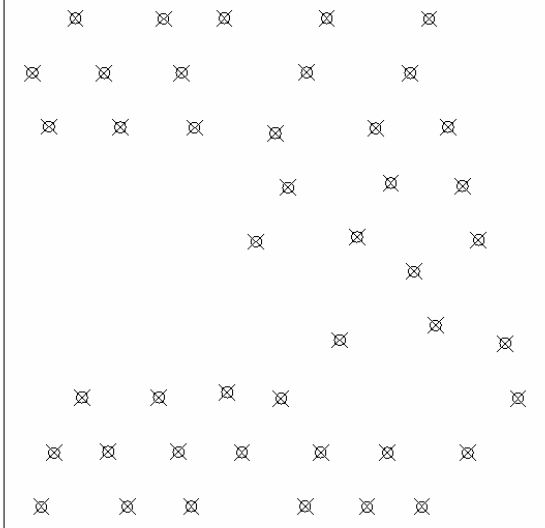
	
<p>Figure 3.10 Sub-optimal layout of the wind farm for Case 1 using WFOG (N44 b)</p>	<p>Figure 3.11 Sub-optimal layout of the wind farm for Case 1 using WFOG (N44 d)</p>
	
<p>Figure 3.12 Sub-optimal layout of the wind farm for Case 1 using WFOG (N44 e)</p>	

Table 3.3 Results for sub-optimal layouts from WFOG for Case 1

	WFOG (N44b)	WFOG (N44d)	WFOG (N44e)
Number of Turbines	44	44	44
Total Power (kW)	21708	21843	21812
Objective function value (1/kW)	1.3745×10^{-3}	1.3660×10^{-3}	1.3680×10^{-3}
Efficiency (%)	95.170	95.762	95.626

3.2 Case 2: Constant Wind Speed and Variable Wind Direction

In this case, the wind is assumed to come from all directions with equal probability at a constant speed of 12 m/s. To simulate this case in WFOG, wind direction is discretized in 36 segments of 10° each.

3.2.1 Results from previous studies

This case was attempted by Mosetti et al. [18] and Grady et al. [19] only. The optimal configurations and the results from earlier studies are presented in figure 3.13 and 3.14 and table 3.4.

As the wind comes with same speed from all the directions, the distance among the wind turbines is the main factor affecting the efficiency of the wind farm and the wake losses in the wind farm. The two layouts presented in figures 3.13 and 3.14 have different characteristics. Mosetti et al.'s layout has sparse placement of wind turbines whereas, in Grady et al.'s layout, wind turbines are densely placed. In Mosetti et al.'s layout, most of the wind turbines are placed on the outer perimeter of the wind farm with few wind turbines in the center part of the wind farm. This layout has 19 wind turbines with the efficiency close to 94 %. The reason for high efficiency is that the distance between the wind turbines is large compared to the Grady et al.'s layout.

The above configurations obtained by Mosetti et al., and Grady et al. were recomputed using WFOG and the findings are presented alongside the reported results in

table 3.4. Mosetti et al.'s results appear to be correct, however, an inconsistency in Grady et al.'s result is noted. The total power production reported is 17220 kW whereas, on recomputing using WFOG, power produced was found to be 13484 kW only. The cause of this discrepancy is likely a data entry error in the manuscript.

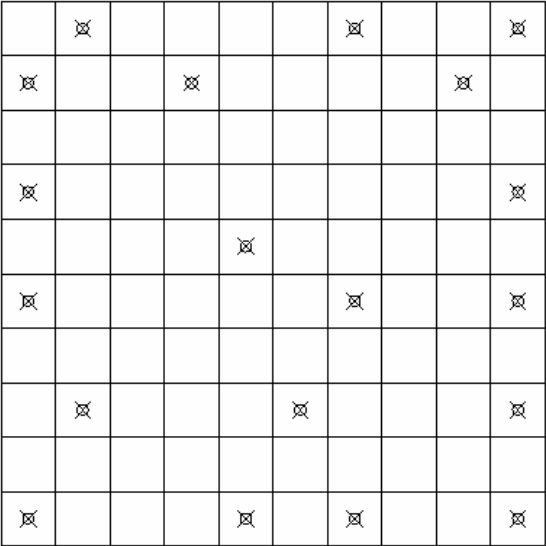
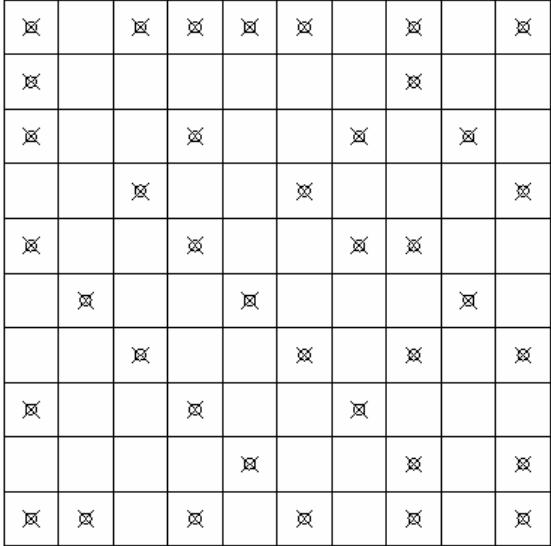
	
Figure 3.13 Mosetti et al.'s optimal layout for Case 2 (after Mosetti et al.)	Figure 3.14 Grady et al.'s optimal layout for Case 2 (after Grady et al.)

Table 3.4 Case 2: Previous studies: reported results and recomputed using WFOG

	Mosetti et al.		Grady et al.	
	Reported	WFOG	Reported	WFOG
Number of Turbines	19	19	39	39
Total Power (kW)	9244	9264	17220	13484
Objective function value (1/kW)	1.7371×10^{-3}	1.7320×10^{-3}	1.5666×10^{-3}	1.9965×10^{-3}
Efficiency (%)	93.851	94.054	92.174	66.694

3.2.2 Results from WFOG with fine grid spacing

For optimizations done on a finely spaced grid, the grid spacing is kept at 1 m. WFOG was run with MATLAB's 'ga' solver to obtain objective function values for different N_t , (number of wind turbines). The graph in figure 3.15 shows the objective function value as a function of the number of wind turbines, N_t . For each data point, the objective function value is the minimum value obtained out of the several runs of 'ga' solver. From the graph in figure 3.15, it is seen that as the number of wind turbines is increased from 15, the cost per unit power decreases. This can be attributed to the fact that as the number of wind turbines increases, the average cost of one wind turbine is reduced.

However, if the number of wind turbines is increased beyond 38 wind turbines, the cost per unit power starts to increase. This is because as more and more wind turbines are placed in a wind farm, wake losses increase and, at some point, the addition of more wind turbines is no longer economical. This trend in figure 3.15 was also observed in case 1 (Figure 3.8). In this case, the minimum cost per unit power (objective function value) is found to be 1.5273×10^{-3} for 38 wind turbines. The optimal layout of these 38 wind turbines is shown in figure 3.16. This configuration produces 17259 kW power (see table 3.5) at an efficiency of 87.6 %. The wind turbines are spread evenly over the entire wind farm with a large inter-turbine spacing. The empty regions observed in optimal configurations in case 1 (Figures 3.9 – 3.12), are absent. This is because the wind comes from all directions (whereas in case 1 the wind was unidirectional).

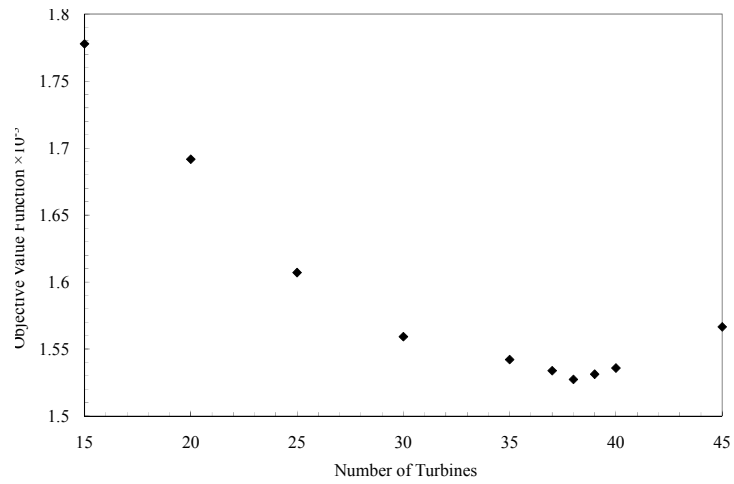


Figure 3.15 Objective function values for different N_t for Case 2

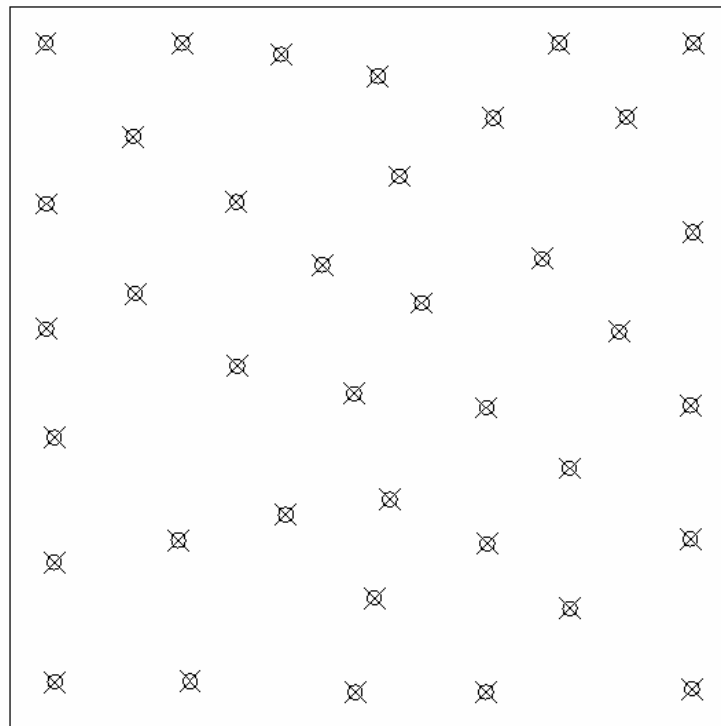


Figure 3.16 Optimal layout for Case 2 with fine grid spacing using WFOG

Table 3.5 Results from WFOG for Case 2

	WFOG	WFOG (optimal)
Number of Turbines	20	38
Total Power (kW)	9847	17259
Objective function value (1/kW)	1.6916×10^{-3}	1.5273×10^{-3}
Efficiency (%)	94.974	87.612

Upon comparison of WFOG's results with Mosetti et al.'s results, it is evident that due to increased flexibility in placing the wind turbines (due to reduced grid spacing of 1 m) 19 more wind turbines can be placed within the boundaries of the wind farm. Even though efficiency of the optimal wind farm has reduced to 87.6 % as compared to 94.0 % reported by Mosetti et al., wind farm efficiency is not a criterion in the optimization process. The optimization process is entirely based on an objective function value (cost per unit power) and WFOG results show that the objective function value is reduced to 1.5273×10^{-3} as compared to 1.7320×10^{-3} (computed using WFOG from Mosetti et al.'s optimal configuration) or 1.7371×10^{-3} (reported by Mosetti et al.).

Moreover, from the graph in figure 3.15, the objective function value for 20 wind turbines is 1.6916×10^{-3} which is lower than the value reported by Mosetti et al. The optimal configuration of these 20 wind turbines produces 9847 kW power (table 3.5) as compared to 9264 kW produced by Mosetti et al.'s layout. The wind farm of these 20 wind turbines operates at an efficiency of 94.9 % whereas Mosetti et al.'s wind farm operates at an efficiency of 94.0 %.

This reinforces the fact that by reducing the grid spacing to 1 m, there is more flexibility in placing the wind turbines which leads to increased efficiency of the wind farm and the opportunity to place more wind turbines in the available space. (Instead of 19, 20 wind turbines can be placed in the same space, which produce more power at a higher efficiency)

3.3 Case 3: Variable Wind Speed and Variable Wind Direction

This is a more realistic case where wind speed and wind direction, both are variable. For the purpose of present study, three different wind speeds (8 m/s, 12 m/s and 17 m/s) are considered, though, WFOG can accept any number of wind speeds. The wind direction is discretized in 36 segments of 10° each (as in previous case). It is not necessary to discretize in 36 segments and more number of segments can be used for more accurate results, though, it should be noted that this will lead to increased computational time. E.g. Discretizing in 72 segments doubles the computational time. The probability or fraction of occurrence of each wind speed from each angle is shown in figure 3.17. It shows that higher wind speeds with high probability of occurrence are available from 270° till 350° .

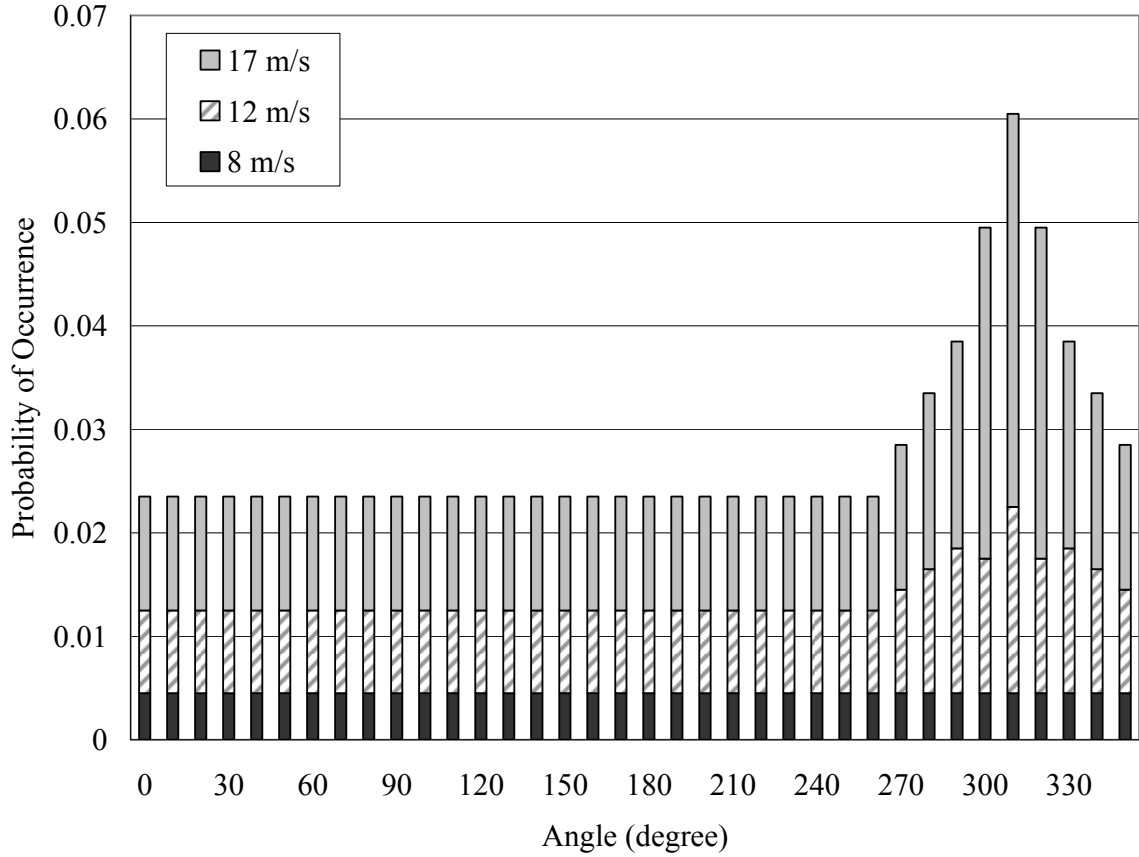


Figure 3.17 Wind distribution for Case 3

3.3.1 Results from previous studies

The case of variable wind speed and direction was attempted by Mosetti et al. [18] and Grady et al. [19]. The optimal configurations and results from these studies are presented in figure 3.18 and 3.19 and table 3.8. Mosetti et al.'s configuration of 15 wind turbines is reported to produce 13460 kW whereas Grady's configuration of 39 wind turbines is reported to produce 32038 kW.

As mentioned earlier (Chapter 2), measurement direction of the angle is not specified in previous studies. In WFOG, the clockwise angular direction is specified as

positive. WFOG was used to analyze the optimal configurations from earlier studies and to avoid confusion, both clockwise and counter clockwise angle measurement directions are considered in separate analyses and results are presented in table 3.9.

The layout reported by Mosetti et al. has only 15 wind turbines and resulted in lower wake losses. The efficiency of the wind farm is close to 95 %. On the other hand, Grady et al.'s layout has 39 wind turbines and is densely packed. This can be explained by the fact that this wind farm operates at an efficiency of mere 54 %, i.e. 46 % of the energy that can be converted to useful power is dissipated due to wake losses. Moreover, on comparing the cost per unit power for the two wind farms, the difference is very large as Mosetti et al.'s wind farm produces power at 1.0046×10^{-3} cost per unit power while Grady's wind farm produces at 1.3660×10^{-3} , 35.9 % costly.

As in case 2 also, a discrepancy in results reported by Grady et al. and computed using WFOG is observed. For this case he reported a power output of 32038 kW. With WFOG, a power output of 19434 kW was obtained for the same wind farm layout (Table 3.6). In contrast, results reported by Mosetti are consistent with those found using WFOG (Table 3.6).

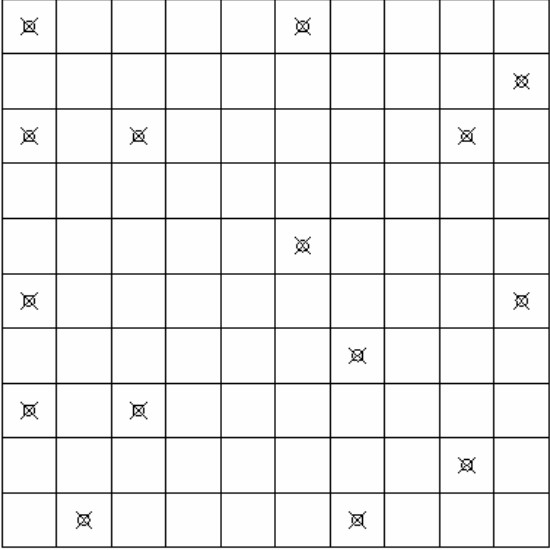
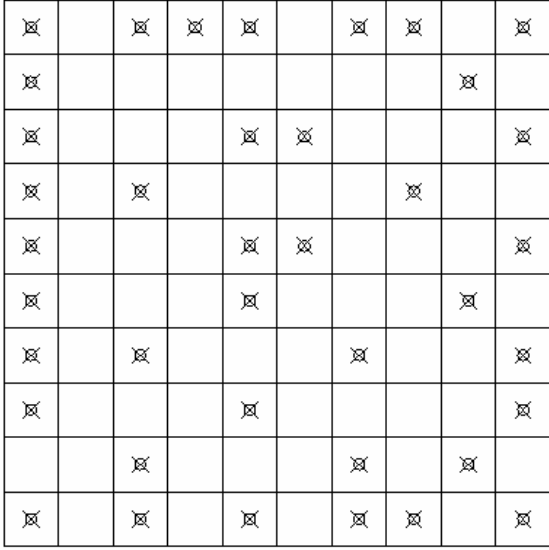
	
Figure 3.18 Mosetti et al.'s optimal layout for Case 3 (after Mosetti et al.)	Figure 3.19 Grady et al.'s optimal layout for Case 3 (after Grady et al.)

Table 3.6 Case 3: Previous studies: reported results and recomputed using WFOG

	Mosetti et al.		
	Reported	WFOG (cw)	WFOG (ccw)
Number of Turbines	15	15	15
Total Power (kW)	13460	13325	13319
Objective function value (1/kW)	9.9405×10^{-4}	1.0041×10^{-3}	1.0046×10^{-3}
Efficiency (%)	94.62	94.968	94.925

	Grady et al.		
	Reported	WFOG (cw)	WFOG (ccw)
Number of Turbines	39	39	39
Total Power (kW)	32038	19434	19708
Objective function value (1/kW)	8.0314×10^{-4}	1.3853×10^{-3}	1.3660×10^{-3}
Efficiency (%)	86.619	53.272	54.023

3.3.2 Results from WFOG with fine grid spacing

As was established in earlier sections, reducing the grid spacing improves the power production and efficiency of the wind farm, in this case, WFOG is utilized for optimization with refined grid spacing of 1 m.

The graph in figure 3.20 shows the objective function value plotted against the number of wind turbines. The trend, as was observed in case 1 and case 2, is observed in this graph also. The cost per unit power for the wind farm reduces as N_t is increased from 15 and increases if N_t is increased beyond 41. The minimum cost per unit power is -

8.4379×10^{-4} for 41 wind turbines. The layout of these 41 wind turbines is shown in figure 3.21. This layout produces 33262 kW power at an efficiency of 86.7 % (see table 3.7).

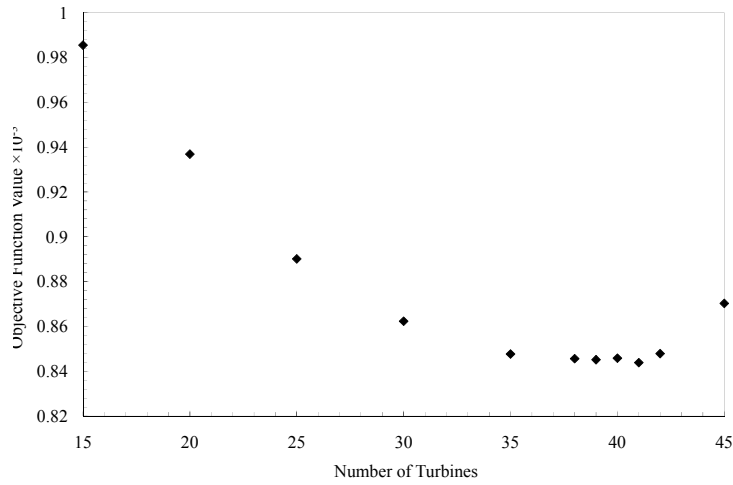


Figure 3.20 Objective function values for different N_t for Case 3

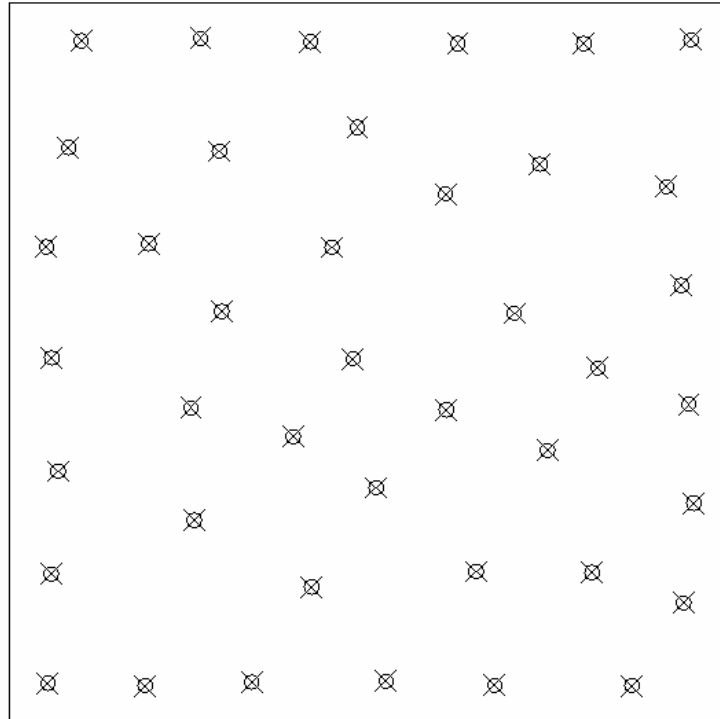


Figure 3.21 Optimal layout for Case 3 with fine grid spacing using WFOG

Table 3.7 Results from WFOG for Case 3

	WFOG	WFOG (optimal)
Number of Turbines	15	41
Total Power (kW)	13563	33262
Objective function value (1/kW)	9.8652×10^{-4}	8.4379×10^{-4}
Efficiency (%)	96.664	86.729

On comparing WFOG's results with those of Mosetti et al.'s, we see that 26 more wind turbines can be placed in the same area (15 wind turbines in Mosetti et al.'s layout and 41 wind turbines in WFOG's optimal layout). The optimal layout produces 33262 kW which is 19937 kW more than the Mosetti et al.'s 13325 kW calculated power output. The efficiency of the optimal wind farm is only 86.7 % which is considerably lower than the value of 94.9% obtained by Mosetti et al.'s. However, the efficiency of the wind farm is not a criterion in the optimization process and only the cost per unit power is optimized which in this case was reduced from 1.0041×10^{-3} to 8.4379×10^{-4} .

Moreover, from graph in figure 3.20, objective function value for 15 wind turbines is 9.8652×10^{-4} which is lower than the value reported by Mosetti et al. The optimal configuration of these 15 wind turbines produces 13563 kW power (table 3.7) as compared to 13325 kW produced by Mosetti et al.'s layout. The wind farm of these 15 wind turbines operates at an efficiency of 96.6 %, slightly higher than that in the optimum configuration calculated by Mosetti et al.

This result reinforces the idea that by reducing the grid spacing to 1 m, the flexibility in placing the wind turbines is higher. Furthermore a larger number of admissible turbine configurations are possible as well as increased efficiency of the optimal wind farm layouts relative to the optimal layouts obtained with coarser grids. Furthermore, the increased flexibility in placement reveals that more turbines can be placed in the available space than would be predicted if placement is constrained to take place on a coarser mesh.

Chapter 4

Conclusions and Recommendations

4.1 Conclusions

In the present study, a code ‘WFOG’ is developed for optimizing the placement of wind turbines in wind farms. Three different wind regimes are selected and optimal layouts obtained for each regime.

WFOG results are compared with results from earlier studies and significant improvements are evident in the results obtained using WFOG. The cost per unit power, which is the objective function, is reduced by 11.7 % for Case 1, 11.8 % for Case 2, and 15.9 % for Case 3 as compared to the cost per unit power values for optimal layouts obtained in earlier studies. It is also observed that the use of fine grid spacing (1 m in WFOG) provides more flexibility in placing the wind turbines. As a result, more wind turbines can be placed in a given space producing more power at a higher efficiency.

4.2 Recommendations

The results obtained in this study motivate to further develop WFOG and investigate the following:

- Performance of different wake models and their validation – There are various wake models discussed in Chapter 1 varying in complexities. These should be tested with

WFOG to assess their effect on results and validation should be carried out using data from a wind farm to find out which ones are better.

- Effect of Turbulence – Atmospheric turbulence affects the wake recovery. The contribution of atmospheric turbulence and turbulence generated due to the wind turbine should be incorporated.
- Wake Interaction – In the present wake model, the wake interaction is not taken into account. This becomes very important in large wind farms where wakes interact and wake recovery slows down as a result.
- Effect of ground – As the wake expands, it encounters ground (water surface in case of offshore wind farms) and can not expand further in that direction. This slows the wake recovery and should be modeled in WFOG.
- Variable hub height of the wind turbines – In the present study, hub height of the wind turbines is fixed and can not be varied. This can be varied to improve the performance of the wind farms and should be further investigated as increasing the hub height might increase the cost of the wind farm.
- Terrain – In the present study, it is assumed that the terrain is flat and is characterized by the surface roughness. A more detailed modeling of the terrain should be incorporated to take into account the effect of very rough terrain which is sometimes encountered for onshore sites.

Appendix A

Coordinates of the wind turbines for the layouts obtained using WFOG

Case 1: Constant Wind Speed and Fixed Wind Direction

The table below gives the abscissas and ordinates of all the wind turbines in the layout shown in figure 3.9.

S. No.	X coordinate	Y coordinate
1	1192	101
2	267	102
3	1747	105
4	1416	106
5	551	113
6	171	301
7	1813	305
8	1511	313
9	982	315
10	1249	340
11	499	364
12	1900	504
13	931	513

14	1604	558
15	640	590
16	1303	615
17	436	636
18	100	646
19	868	753
20	1652	760
21	385	880
22	1070	890
23	725	1084
24	1127	1197
25	1393	1265
26	195	1336
27	781	1379
28	1534	1472
29	516	1490
30	1821	1498
31	983	1499
32	1187	1528
33	289	1595
34	1471	1671
35	567	1689
36	1770	1697

37	934	1700
38	108	1887
39	621	1889
40	887	1899
41	1893	1899
42	1294	1900
43	1631	1900
44	402	1900

Case 2: Constant Wind Speed and Variable Wind Direction

The table below gives the abscissas and ordinates of all the wind turbines in the layout shown in figure 3.16.

S. No.	X coordinate	Y coordinate
1	100	101
2	480	101
3	1527	101
4	1900	102
5	754	132
6	1023	193
7	1714	307
8	1343	308
9	344	360

10	1083	470
11	630	541
12	102	546
13	1899	625
14	1480	699
15	869	716
16	350	795
17	1145	821
18	102	893
19	1694	901
20	633	996
21	957	1073
22	1892	1106
23	1325	1111
24	124	1194
25	1556	1280
26	1056	1366
27	767	1407
28	1892	1476
29	469	1479
30	1327	1488
31	124	1540
32	1014	1639

33	1557	1668
34	501	1870
35	126	1872
36	1896	1891
37	1323	1900
38	960	1900

Case 3: Variable Wind Speed and Variable Wind Direction

The table below gives the abscissas and ordinates of all the wind turbines in the layout shown in figure 3.21.

S. No.	X coordinate	Y coordinate
1	531	100
2	1893	104
3	199	107
4	836	110
5	1245	115
6	1595	115
7	966	348
8	163	404
9	583	414
10	1473	450
11	1825	513

12	1211	533
13	387	672
14	102	680
15	896	681
16	1866	787
17	589	859
18	1402	865
19	117	989
20	954	991
21	1634	1017
22	1887	1118
23	504	1128
24	1213	1133
25	788	1208
26	1494	1246
27	135	1304
28	1018	1350
29	1900	1393
30	513	1440
31	1296	1583
32	1617	1585
33	116	1589
34	839	1626

35	1872	1670
36	1045	1888
37	673	1890
38	106	1893
39	1347	1899
40	377	1900
41	1729	1900

Appendix B

Derivation of the Jensen's Wake model

The analytical wake model utilized in this study is derived by conserving momentum across a control volume in the wake of a wind turbine. The control volume is shown in figure B.1. The contribution from the tip vortices is neglected so that the wake can be treated as a turbulent wake [7, 8]. A balance of momentum across the control volume gives

$$\pi r_d^2 u_1 + \pi (r_1^2 - r_d^2) u_0 = \pi r_1^2 u \quad (\text{B.1})$$

where u_1 is the velocity in the wake just behind the rotor and is $(1 - 2a)u_0$ (according to the Betz theory)

Thus, equation B.1 is

$$\pi r_d^2 (1 - 2a) u_0 + \pi (r_1^2 - r_d^2) u_0 = \pi r_1^2 u \quad (\text{B.2})$$

Also, it is assumed that the wake expands linearly and its radius is given by

$$r_1 = r_d + \alpha x \quad (\text{B.3})$$

where x is the downstream distance from the wind turbine.

Substituting equation B.3 in equation B.2, we get

$$\pi r_d^2 (1-2a)u_0 + \pi \left((r_d + \alpha x)^2 - r_d^2 \right) u_0 = \pi (r_d + \alpha x)^2 u \quad (\text{B.4})$$

On solving for u , equation B.4 reduces to

$$u = u_0 \left[1 - \frac{2ar_d^2}{(r_d + \alpha x)^2} \right] \quad (\text{B.5})$$

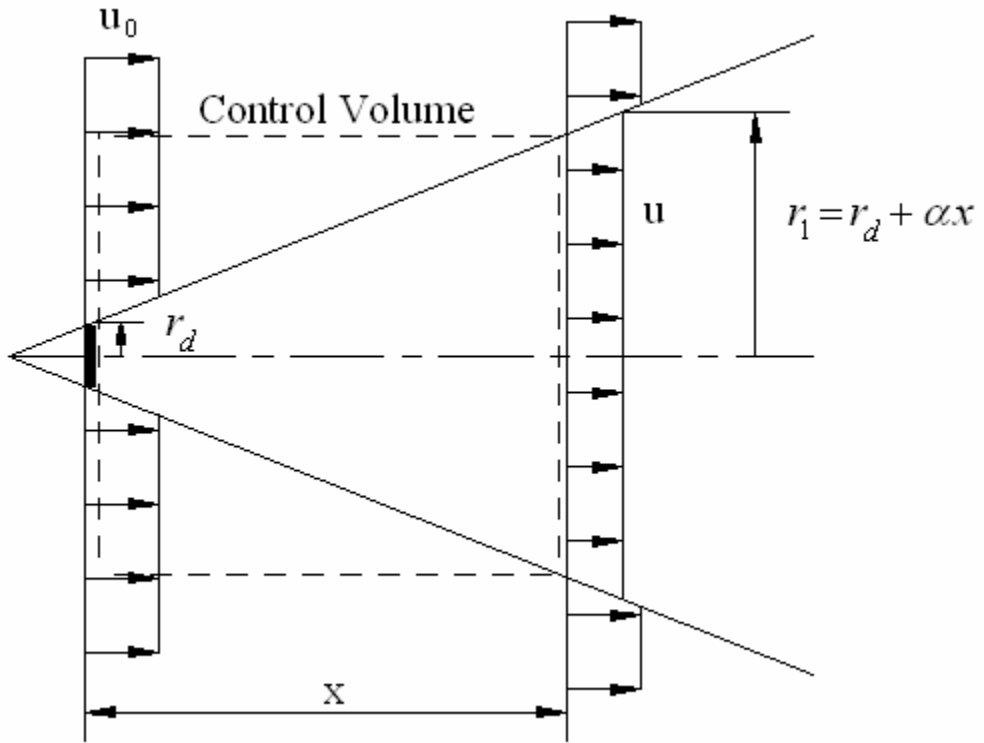


Figure B.1 Wake of a single wind turbine

Appendix C

Source code of WFOG

Source code developed for Case 1 (Optimal layout in figure 3.9)

File Analyse_Grid.m

```
function obj = Analyse_Grid(wf)

global wind_farm;
global N;
global velocity_farm;
N = 30;
wind_farm = zeros(N,2);
velocity_farm = zeros(N,1);
wf = wf * 1000;
wf = round(wf);
for a = 1:1:N
    b = (2 * a) - 1;
    wind_farm(a,1) = wf(b);
    wind_farm(a,2) = wf(b + 1);
end
```



```

power = 0;
total_power = 0;
wind_farm = sortrows(wind_farm,[2 1]);

for i = 1:1:N

    x = wind_farm(i,1);
    y = wind_farm(i,2);

    velocity = check_wake(x,y,i);
    velocity_farm(i) = velocity;
    power = 0.3 * (velocity ^ 3);

    total_power = total_power + power;

end

```

File check_wake.m

```

function f = check_wake(x,y,j)

global wind_farm;

```

```

u0 = 12;

alpha = 0.09437;

rotor_radius = 27.881;

chk = 0;          % chk = 0 No wake----- chk = 1 Wake
chk1 = 0;         % chk1 = 1 Two turbines at same position
counter = 0;

for i = 1:1:j-1

    ydistance = abs(y - wind_farm(i,2));
    xdistance = abs(x - wind_farm(i,1));

    if (ydistance < 199) && (xdistance < 199)

        chk1 = 1;

    end

    radius = rotor_radius + (alpha * ydistance);

    xmin = wind_farm(i,1) - radius;

```

```

xmax = wind_farm(i,1) + radius;

if (xmin < x) && (xmax > x)      % Checking for wake by radius

    % Turbine in wake

    chk = chk + 1;

    %velocity = calculate_velocity(i,j); % Call calculate velocity

    counter = counter + 1;

    location(counter) = i;

else

    % Turbine outside of wake

    chk = chk + 0;

end

end

if chk == 0

    ff = u0;

else

    % Call calculate velocity

```

```

    velocity = calculate_velocity(j,location,counter);

    ff = velocity * u0;

end

```

```

if chk1 == 1

    f = 0;

else

    f = ff;

end

```

File calculate_velocity.m

```

function vel = calculate_velocity(j,location,counter)

global wind_farm;

count = counter;

alpha = 0.09437;

a = 0.326795;

rotor_radius = 27.881;

velr1 = 0;

for lo = 1:1:count-1

```

```

for ii=1:1:counter-1      % Loop for checking turbine 1 by 1

    for jj = ii+1 : 1 : counter

        y1 = location(ii);
        y2 = location(jj);
        ydistance = abs(wind_farm(y1,2) - wind_farm(y2,2));
        radius = rotor_radius + (alpha * ydistance);

        xmin = wind_farm(y2,1) - radius;
        xmax = wind_farm(y2,1) + radius;

        if (xmin < wind_farm(y2,1)) && (xmax > wind_farm(y2,1))

            % Eliminate turbine at ii

            location(ii) = [];

            counter = counter - 1;

            break;
        end
    end
end

```

```

        end

    end

end

for ii=1:1:counter
    y1 = location(ii);
    ydistance = wind_farm(j,2) - wind_farm(y1,2);
    denominator = ((alpha * ydistance / rotor_radius) + 1) ^ 2;
    velr = (1 - (2 * a / denominator));
    velr1 = velr1 + ((1 - velr)^2);

end

vel = 1 - (velr1 ^ 0.5);

```

File LowerBound.m

```
function LB1 = LowerBound(LB)
```

```
N = 60;
```

```
LB1 = zeros(1,N);
```

```
ax = 1;
```

```
LB1(1,:) = ax;
```

File UpperBound.m

```
function UB1 = UpperBound(LB)
```

```
N = 60;
```

```
UB1 = zeros(1,N);
```

```
x = 2.8;
```

```
UB1(1,:) = x;
```

Bibliography

1. Righter RW, 1996. Wind Energy in America: A History. University of Oklahoma Press
2. Burton T, Sharpe D, Jenkins N, Bossanyi E, 2001. Wind Energy Handbook. John Wiley
3. EWEA, 2009. Wind Energy – The Facts. Earthscan
4. Lanchester FW, 1915. Contribution to the theory of propulsion and the screw propeller. Transactions of the Institution of Naval Architects ; LVII: 98–116.
5. Betz A, 1920. Der Maximum der theoretisch mölichen Ausnützung des Windes durch Windmotoren. Zeitschrift für das Gesamte Turbinenwesen ; 26: 307–309
6. Frandsen S, Barthelmie R, Pryor S, Rathmann O, Larsen S, Hojstrup J, Thogersen M, 2006. Analytical Modelling of Wind Speed Deficit in Large Offshore Wind Farms. Wind Energy. Issue 9, 39-53
7. Jensen NO, 1983. A note on Wind Generator Interaction. Riso National Laboratory, Roskilde, Denmark
8. Katic I, Hojstrup J, Jensen NO, 1986. A simple model for cluster efficiency. Proceedings of the European Wind Energy Conference and Exhibition. 407-410.
9. Ishihara T, Yamaguchi A, Fujino Y, 2004. Development of a New Wake Model Based on a Wind Tunnel Experiment. Global Wind Power.
10. Werle MJ, 2008. A New Analytical Model for Wind Turbine Wakes. FloDesign Inc., Wilbraham, MA.

11. Crasto G, Gravdahl AR, 2008. CFD wake modeling using a porous disc. European Wind Energy Conference and Exhibition. Brussels, Belgium
12. Crespo A, Hernandez J, Frandsen S, 1999. Survey of Modelling Methods for Wind Turbine Wakes and Wind Farms. Wind Energy. 1-24.
13. Frandsen S, 1992. On the wind speed reduction in the center of large clusters of wind turbines. Journal of Wind Engineering and Industrial Aerodynamics, Issue 39, 251-265
14. Barthelmie RJ, Folkerts L, Larsen GC, Rados K, Pryor SC, Frandsen ST, Lange B, Schepers G, 2006. Comparison of Wake Model Simulations with Offshore Wind Turbine Wake Profiles Measured with Sodar. Journal of Atmospheric and Oceanic Technology, Issue 7, 888-901
15. Mechali M, Barthelmie R, Frandsen S, Jensen L, Rethore PE, 2006. Wake effects at Horns Rev and their influence on energy production. EWEC 2006 at Athens, Greece, p.10
16. Cleve J, Greiner M, Envoldsen P, Birkemose B, Jensen L, 2009. Model-based Analysis of Wake-flow Data in the Nysted Offshore Wind Farm. Wind Energy, Issue 2, 125-135
17. Beyer HG, Ruger T, Schafer G, Waldl HP, 1996. Optimization of Wind Farm Configurations with Variable Number of Turbines. Proceedings of the European Union Wind Energy Conference (EUWEC), Sweden, 1069-1073
18. Mosetti G, Poloni C, Diviacco B, 1994. Optimization of wind turbine positioning in large windfarms by means of a genetic algorithm. Journal of Wind Engineering and Industrial Aerodynamics, Issue 51, 105-116

19. Grady SA, Hussaini MY, Abdullah MM, 2005. Placement of wind turbines using genetic algorithms. *Renewable Energy*, Issue 30, 259-270
20. Marmidis G, Lazarou S, Pyrgioti E, 2008. Optimal placement of wind turbines in a wind park using Monte Carlo simulation. *Renewable Energy*, Issue 33, 1455-1460
21. Elkinton CN, Manwell JF, McGowan JG, 2008. Algorithms for Offshore Wind Farm Layout Optimization. *Wind Engineering*, Issue 1, 67-83
22. Elkinton CN, Manwell JF, McGowan JG, 2008. Optimizing the Layout of Offshore Wind Energy Systems. *Marine Technological Society Journal*, Issue 2, 19-27
23. Acero JFH, Acevedo JRF, Rendon MV, Oleszewski OP, 2009. Linear Wind Farm Layout Optimization through Computational Intelligence. *Proceedings of the 8th Mexican International Conference on Artificial Intelligence*, 692-703